Module 3:
Signals and Spectra

3.0 Introduction

An understanding of the different types of signals typically present in electrical systems, and the frequency content of such signals is critical to the design of electromagnetically compatible circuits. Many common signals contain high frequency components which may, under certain circumstances, act as sources of interference. Three types of signals will be examined in this module, which are found in many electrical systems. These include narrowband continuous wave (sinusoidal) signals, repetitive broadband signals (such as digital clock signals), and single event broadband signals (such as spark discharges). The emphasis of this module will be to present material required for an understanding of the frequency spectra of these types of signals. In particular, the relationship between rise time, wave shape and spectral content of a signal will be examined.

3.1 Classification of signals

For the purposes of the material presented here, a signal is considered to be either a voltage or current waveform that is described mathematically. Signals may be classified in many ways. A few of the more common classifications are listed below.

- **energy signals**

The instantaneous power dissipated by a voltage *v(t)* in a resistance *R* is given by

$$p(t) = \frac{|v(t)|^2}{R}$$

and for a current *i(t)*

$$p(t) = |i(t)|^2 R .$$

It can be seen that the power in each case is proportional to the squared magnitude of the signal. If these signals are applied to a 1 ohm resistor, then both of the equations above assume the same form. For a general signal *f(t)*

$$p(t) = |f(t)|^2 .$$

The energy associated with this signal during a time interval from t_1 to t_2 is given by

$$E_f = \int_{t_1}^{t_2} |f(t)|^2 dt .$$

A signal whose energy remains finite over an infinite time interval

$$E_f = \int_{-\infty}^{\infty} |f(t)|^2 dt < \infty$$

is referred to as an *energy signal*.

- **power signals**

The average amount of power dissipated by a signal *f(t)* during an interval of time from t_1 to t_2 is

$$P = \frac{1}{(t_2 - t_1)} \int_{t_1}^{t_2} |f(t)|^2 \, dt \, .$$

A signal which satisfies the relationship

$$0 < \lim_{T \to \infty} \frac{1}{T} \int_{-T/2}^{T/2} |f(t)|^2 dt < \infty$$

has finite average power, and is referred to as a *power signal*.

- **deterministic signals**

A signal whose behavior is precisely known is referred to as being *deterministic*. These include sinusoidal signals, and digital clock signals. Usually, such signals can be represented by explicit mathematical expressions.

- **non-deterministic signals**

A signal whose behavior is not known, and which can only be described statistically is referred to as being *non-deterministic*, or *random*. Digital data signals are often non-deterministic.

- **periodic signals**

Repetitive, time-domain signals, such as the clock signals often present in digital devices, are referred to as being *periodic*. A function *f(t)* is said to be periodic if it satisfies the relationship

$$f(t) = f(t \pm n T_0) \qquad for \quad n = 1, 2, 3, ...$$

for every time t, where T_0 is the period of the function. The fundamental angular frequency, ω_o, of a periodic function is

$$\omega_o = 2\pi f_0 = \frac{2\pi}{T_0}.$$

Periodic signals are classified as power signals because their average power is finite.

Sinusoidal signals represent a class of periodic signals that are commonly used in many analysis techniques. These techniques, such as those involving Fourier series, decompose complicated waveforms into a series of sinusoidal waveforms. A sinusoidal waveform *f(t)* is usually represented by

$$f(t) = A\cos(\omega t + \theta)$$

where A is the *amplitude* of the signal, θ is the *phase*, and ω is the *angular frequency* in radians per second ($\omega=2\pi f$).

- **non-periodic signals**

A non-periodic waveform is one that does not satisfy the criteria for a periodic waveform. Non-periodic signals are referred to as energy signals because their total energy is finite.

3.2 The electromagnetic spectrum

In the previous chapter it was seen that, in a source free region, $\vec{E}$ and $\vec{B}$ satisfy homogeneous wave equations. For the case of time harmonic excitation, these equations reduce to homogeneous Helmholtz equations, the solutions of which represent propagating waves. Thus electromagnetic energy is transferred in the form of waves which propagate at velocities that depend on the medium of transmission ($v = 1/\sqrt{\mu\varepsilon}$), and oscillate at frequencies that depend on the nature of the source.

Electromagnetic radiation is typically classified according to frequency or wavelength (although in the range including visible and ultraviolet light, x-rays, and γ-rays, radiation is sometimes classified according to photon energy). The *electromagnetic spectrum*, shown in Figure 1, is divided into frequency and wavelength bands. At the low frequency end lie the radio bands. Above this is the microwave region, which occupies the range from about 1 GHz to the lower infrared band, and contains the UHF, SHF, EHF, and millimeter-wave bands. The so-called *visible spectrum* extends from 4.2×10^{14} Hz (deep red, 720 nm) to 7.9×10^{14} Hz (violet, 380 nm). At higher frequencies lie ultraviolet light, x-rays, and γ-rays.

It is important to note that certain sections of the electromagnetic spectrum are reserved by regulatory agencies such as the FCC. Broadcasts and emissions in these bands are subject to laws and regulations established by such agencies.

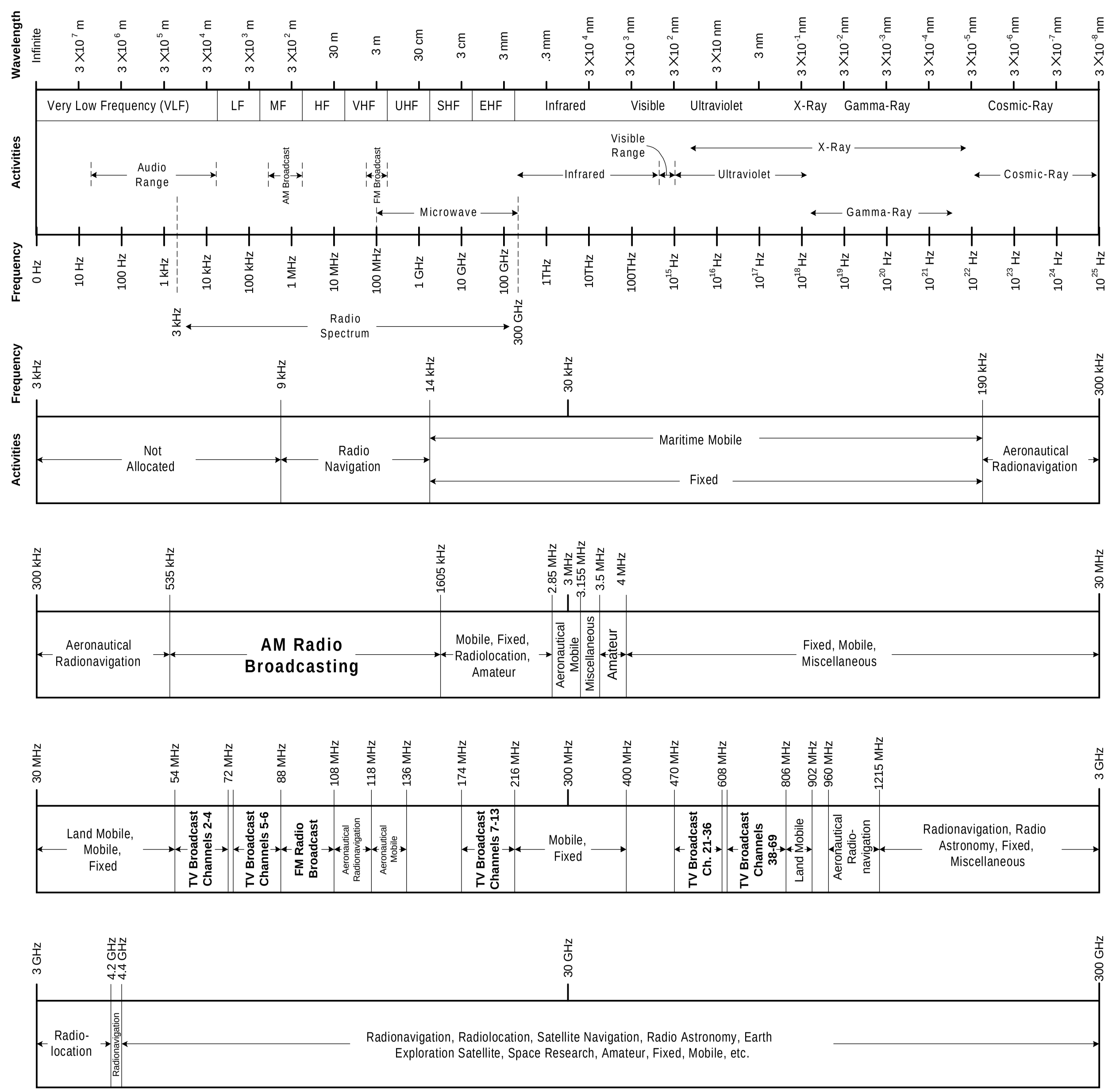

Figure 1. The electromagnetic spectrum.

Microwave frequency band designations

Old	New	Frequency Range (GHz)
Ka	K	26.5 - 40
K	K	20 - 26.5
K	J	18 - 20
Ku	J	12.4 - 18
X	J	10 - 12.4
X	I	8 - 10
C	H	6 - 8
C	G	4 - 6
S	F	3 - 4
S	E	2 - 3
L	D	1 - 2
UHF	C	0.5 - 1

3.3 Series expansions and basis functions

Complex signals which are periodic can be represented as linear combinations of simpler signals known as *basis functions*. Thus a periodic signal *f(t)* with period *T* may be represented

$$f(t) = \sum_{n=0}^{\infty} c_n \varphi_n(t)$$

$$= c_0\varphi_0(t) + c_1\varphi_1(t) + c_2\varphi_2(t) + \ldots$$

where the functions $\varphi_n(t)$ are periodic, having the same period as *f(t)*, and the coefficients c_n are referred to as *expansion coefficients*. The best choice of basis functions depends on the signal *f(t)* that is to be represented.

- **orthogonality of basis functions**

Regardless of the type of basis function selected, the process of determining the expansion coefficients c_n is greatly simplified if the basis functions possess the property

$$\int_{t_1}^{t_1+T} \varphi_n(t)\varphi_m^*(t)\,dt = \begin{cases} \alpha_m & for\ \ m = n \\ 0 & for\ \ m \neq n \end{cases}$$

where * indicates the complex conjugate. A set of functions $\varphi_n(t)$ having this property is said to be *orthogonal*. If both sides of the signal expansion above are multiplied by $\varphi_m^*(t)$, and then integrated over time interval *T*, it is seen that

$$\int_{t_1}^{t_1+T} \varphi_m^*(t) f(t)\, dt = \sum_{n=0}^{\infty} c_n \int_{t_1}^{t_1+T} \varphi_m^*(t)\, \varphi_n(t)\, dt$$

$$= c_m \alpha_m$$

or

$$c_n = \frac{1}{\alpha_n} \int_{t_1}^{t_1+T} \varphi_n^*(t) f(t) dt .$$

This type of signal expansion, using a series of basis functions to represent a more complex signal, is useful to mathematicians and engineers because the response of a linear system to a complex periodic signal can be determined by finding the linear superposition of the responses to much simpler inputs. This representation is useful to EMC engineers for a slightly different reason, however. If the basis functions are chosen correctly, this series expansion corresponds to a complex signal composed of many individual single frequency signals. Thus a square wave, like a digital clock signal, can be thought of as being composed of many components of different frequencies, each oscillating at some integer multiple of a fundamental frequency f_0, any one of which may potentially "escape" and act as a source of interference. All that is left is to select basis functions which will form a series that properly represents a particular signal.

3.4 Fourier series

The most common series representation of periodic signals is a *trigonometric Fourier series*. This type of series uses sinusoidal basis functions, such that

$$\varphi_n(t) = 1 \quad \ldots\ for\ \ n = 0$$

and

$$\varphi_n(t) = \begin{cases} \cos(n\omega_o t) \\ \sin(n\omega_o t) \end{cases} \quad \ldots\ for\ \ n = 1, 2, 3\, ,$$

where $\omega_0 = \dfrac{2\pi}{T}$.

Thus a periodic signal *f(t)* with period *T* may be represented as

$$f(t) = a_0 + \sum_{n=1}^{\infty} a_n \cos(n\omega_o t) + \sum_{n=1}^{\infty} b_n \sin(n\omega_o t)$$

where

$$a_o = \frac{1}{T}\int_{t_1}^{t_1+T} f(t)\,dt$$

$$a_n = \frac{2}{T}\int_{t_1}^{t_1+T} f(t)\cos(n\omega_o t)\,dt$$

and

$$b_n = \frac{2}{T}\int_{t_1}^{t_1+T} f(t)\sin(n\omega_o t)\,dt\,.$$

Here a_0 is the *average value* of the signal, the terms for which n=1 are referred to as *fundamental frequency* terms, and the terms for which n>1 are referred to as *harmonic* terms.
It is seen that the fundamental terms have frequency f_0 = 1/T, while the second harmonic terms have frequency $2f_0$ = 2/T, the third harmonic terms have frequency $3f_0$ = 3/T, and the n^{th} harmonic terms have frequency $nf_0 = n$/T.

The a_n and b_n terms of the Fourier series are found using the following orthogonality properties:

$$\int_{t_1}^{t_1+T} \sin(n\omega_o t)\cos(m\omega_o t)\,dt = 0$$

$$\int_{t_1}^{t_1+T} \sin(n\omega_o t)\sin(m\omega_o t)\,dt = \int_{t_1}^{t_1+T} \cos(n\omega_o t)\cos(m\omega_o t)\,dt = \begin{cases} 0 & for\ n \neq m \\ \frac{T}{2} & for\ n = m \end{cases}.$$

- **complex exponential Fourier series**

An equivalent and more useful form of the Fourier series discussed above can be obtained by applying *Euler's identity*

$$e^{jn\omega t} = \cos(n\omega t) + j\sin(n\omega t)$$

This gives

$$\cos(n\omega t) = \frac{e^{jn\omega t} + e^{-jn\omega t}}{2}$$

and

$$\sin\omega t = \frac{e^{j\omega t} - e^{-j\omega t}}{2j}.$$

When expressed in complex exponential form, the basis functions are

$$\varphi_n(t) = e^{jn\omega_o t} \quad for\ n = -\infty, ..., -1, 0, 1, ..., \infty$$

and have the orthogonality property

$$\int_{t_1}^{t_1+T} e^{-jm\omega_o t} e^{jn\omega_o t} dt = \begin{cases} 0 & for\ n \neq m \\ T & for\ n = m \end{cases}.$$

Using exponential basis functions, a periodic signal *f(t)* of period *T* may be expressed

$$f(t) = \sum_{n=-\infty}^{\infty} c_n e^{jn\omega_o t}.$$

Multiplying both sides of this expression by $\varphi_m^*(t) = e^{-jm\omega_o t}$ and integrating over a period T results in

$$\int_{t_1}^{t_1+T} e^{-jm\omega_o t} f(t) dt = \sum_{n=-\infty}^{\infty} c_n \int_{t_1}^{t_1+T} e^{-jm\omega_o t} e^{jn\omega_o t} dt$$

which after application of the orthogonality relation yields

$$\int_{t_1}^{t_1+T} e^{-jm\omega_o t} f(t) dt = c_m T.$$

From this the expansion coefficients are found to be

$$c_n = \frac{1}{T} \int_{t_1}^{t_1+T} f(t) e^{-jn\omega_o t} dt.$$

It is often easier to compute these expansion coefficients of the complex exponential Fourier series, than the coefficients of the trigonometric Fourier series.

It can be seen that the complex exponential Fourier series contains both positive-valued harmonic frequencies (ω_o, $2\omega_o$, $3\omega_o$, ...) and negative-valued harmonic frequencies ($-\omega_o$, $-2\omega_o$, $-3\omega_o$, ...). Also the expansion coefficients of the complex Fourier series may themselves be complex, while the expansion coefficients of the trigonometric Fourier series are real valued. The expansion coefficients associated with the positive and negative harmonic frequencies are conjugates of each other

$$c_{-n} = \frac{1}{T}\int_{t_1}^{t_1+T} f(t)\,e^{jn\omega_o t}dt$$

$$= c_n^* \,.$$

The complex exponential Fourier series representation of *f(t)* may be written

$$f(t) = c_o + \sum_{n=1}^{\infty} c_n e^{jn\omega_o t} + \sum_{n=-1}^{-\infty} c_n e^{jn\omega_o t}$$

Switching the indices of the second summation to positive values then gives

$$f(t) = c_o + \sum_{n=1}^{\infty} c_n e^{jn\omega_o t} + \sum_{n=1}^{\infty} c_n^* e^{-jn\omega_o t}$$

$$= c_o + \left(\sum_{n=1}^{\infty} c_n e^{jn\omega_o t}\right) + \left(\sum_{n=1}^{\infty} c_n e^{jn\omega_o t}\right)^* = c_o + 2\,\mathrm{Re}\left\{\sum_{n=1}^{\infty} c_n e^{jn\omega_o t}\right\}$$

$$= 2\,\mathrm{Re}\left\{\sum_{n=0}^{\infty} c_n e^{jn\omega_o t}\right\} = \sum_{n=0}^{\infty} 2\,\mathrm{Re}\left\{(c_{n_r} + jc_{n_i})(\cos(n\omega_o t) + j\sin(n\omega_o t))\right\}$$

$$= \sum_{n=0}^{\infty} 2\left[c_{n_r}\cos(n\omega_o t) - c_{n_i}\sin(n\omega_o t)\right]$$

$$= \sum_{n=0}^{\infty} a_n\cos(n\omega_o t) + \sum_{n=0}^{\infty} b_n\sin(n\omega_o t)$$

where

$$a_n = 2c_{n_r}, \quad \text{and } b_n = -2c_{n_i}.$$

- **justification for use of complex-exponential Fourier series**

How do we know that a complex exponential Fourier series like the one presented above is an accurate representation of a signal? Let $S_n(t)$ be an approximation of a periodic function $f(t)$ with period T. $S_n(t)$ is a $2n+1$ term sum of exponentials

$$S_n(t) = c_{-n}e^{-jn\omega_o t} + \ldots + c_{-2}e^{-j2\omega_o t} + c_{-1}e^{-j\omega_o t} + c_0 + c_1 e^{jt} + c_2 e^{j2\omega_o t} + \ldots + c_n e^{jn\omega_o t}$$

$$= \sum_{m=-n}^{n} c_m e^{jm\omega_o t}.$$

The error of this approximation can be defined as

$$\varepsilon_n(t) = f(t) - S_n(t).$$

Therefore, the approximation, $S_n(t)$, is equal to the original function, $f(t)$, minus an error term. The mean square error is defined as

$$M = \frac{1}{T}\int_{-T/2}^{T/2} \varepsilon_n^2(t)\,dt.$$

To improve the accuracy of $S_n(t)$, the coefficients c_m are chosen in such a way that M is a minimum. From the expression above, it is seen that

$$M = \frac{1}{T}\int_{-T/2}^{T/2} \left(f(t) - S_n(t)\right)^2 dt$$

or

$$M = \frac{1}{T}\int_{-T/2}^{T/2} \left(f(t) - \sum_{m=-n}^{n} c_n e^{jm\omega_o t}\right)^2 dt.$$

The term M is minimized by setting the derivative of M with respect to c_n equal to zero

$$\frac{\partial M}{\partial c_l} = \frac{1}{T}\int_{-T/2}^{T/2} 2\left[f(t) - \sum_{m=-n}^{n} c_n e^{jm\omega_o t}\right]\cdot\left(-e^{jl\omega_o t}\right)dt = 0$$

where $l = -n, ..., -2, -1, 0, 1, 2, ..., n$. This gives

$$\int_{-T/2}^{T/2} f(t)e^{jl\omega_o t}dt = \sum_{m=-n}^{n} c_n \left(\int_{-T/2}^{T/2} e^{jm\omega_o t}e^{jl\omega_o t}dt\right) .$$

Using the following orthogonality relationship (where l and n are integers)

$$\int_{-T/2}^{T/2} e^{jl\omega_o t} e^{-jm\omega_o t}dt = \begin{cases} 0 & ...\ l \neq m \\ T & ...\ l = m \end{cases}$$

the Fourier coefficient c_l is found to be

$$c_l = \frac{1}{T}\int_{-T/2}^{T/2} f(t)e^{-jl\omega_o t}dt .$$

It can be shown that as n approaches infinity, the error term M goes to zero. Thus, any function satisfying certain conditions (to be discussed in the next subsection) can be represented by an infinite Fourier series.

$$f(t) = \sum_{n=-\infty}^{\infty} c_n e^{jn\omega_o t} .$$

- **existence of the Fourier series**

The existance of a convergent Fourier series is guaranteed if the function *f(t)* satisfies the *Dirichlet conditions*:

– *f(t)* is absolutely integrable over one period (*weak Dirichlet condition*)

$$\int_{t_1}^{t_1+T} |f(t)|\, dt < \infty$$

– *f(t)* is finite for all *t* in a period T_0

– *f(t)* has a finite number of maxima and minima in a period T_0

– *f(t)* has a finite number of discontinuities in a period T_0

If the requirements above are satisfied, the existence of a convergent Fourier series is guaranteed.

- **properties of Fourier coefficients**

Direct computation of the expansion coefficients for the trigonometric and complex exponential Fourier series discussed in the sections above can prove difficult for certain waveforms. For *piecewise linear* waveforms, certain properties of the Fourier series can be exploited to make this less difficult.

– **linearity**

A waveform may be expressed as a linear combination of two or more functions

$$f(t) = a_1 x_1(t) + a_2 x_2(t) + a_3 x_3(t) + \ldots.$$

As a result, the Fourier series representation of *f(t)* can be written as a linear combination of the Fourier series representations of $x_1(t),\ x_2(t),\ x_3(t),\ \ldots$, etc.

$$f(t) = a_1 \sum_{n=-\infty}^{\infty} c_{1n} e^{jn\omega_o t} + a_2 \sum_{n=-\infty}^{\infty} c_{2n} e^{jn\omega_o t} + a_3 \sum_{n=-\infty}^{\infty} c_{3n} e^{jn\omega_o t} + \ldots.$$

$$= \sum_{n=-\infty}^{\infty} [\, a_1 c_{1n} + a_2 c_{2n} + a_3 c_{3n} + \ldots \,]\, e^{jn\omega_o t}$$

– **time-shifting**

The Fourier coefficients of a waveform *f(t)* that has been shifted forward or backward in time by an amount α can be found directly from the expansion coefficients of *f(t)*. The Fourier series representation of a time-shifted waveform is

$$f(t \pm \alpha) = \sum_{n=-\infty}^{\infty} c_n e^{jn\omega_o (t \pm \alpha)}$$

$$= \sum_{n=-\infty}^{\infty} c_n e^{\pm jn\omega_o \alpha} e^{jn\omega_o t} .$$

Thus it can be seen that the expansion coefficients of $f(t \pm \alpha)$ can be obtained by multiplying the expansion coefficients of $f(t)$ by $e^{\pm jn\omega_o \alpha}$.

– **unit impulse function**

A third important property of Fourier series involves the so called *unit impulse function* δ(t). This function is defined such that

$$\delta(t) = \begin{cases} 0 & \text{... for } t < 0 \\ 0 & \text{... for } t > 0 \end{cases}$$

or

$$\delta(t) = 0 \quad \dots \quad t \neq 0$$

and

$$\int_{\tau-\Delta}^{\tau+\Delta} \delta(t-\tau) f(t)\, dt = f(\tau) \quad \dots \forall \quad \Delta > 0$$

where 0^- and 0^+ are infinitely small intervals of time just before and after t=0, respectively. This function is zero everywhere except at t=0, where it takes on an undefined value. The unit impulse may be thought of as having zero width and infinite height, and is usually represented by a vertical arrow when plotted.

As an example, consider a signal which consists of a periodic train of impulse functions

$$f(t) = \sum_{k=-\infty}^{\infty} \delta(t + kT).$$

The Fourier expansion coefficients associated with this signal are

$$c_n = \frac{1}{T} \int_{-T/2}^{T/2} \delta(t) e^{-jn\omega_o t} dt = \frac{1}{T}.$$

If $f(t)$ is shifted by an amount of time $\pm\alpha$, the expansion coefficients are

$$c_n = \frac{1}{T} e^{\pm jn\omega_o\alpha}.$$

– **differentiation property**

The Fourier coefficients c_n, can be found by using a property of the Fourier series involving the derivatives of *f(t)*. The Fourier coefficient of the i^{th} derivative of c_n, has a simple relationship with c_n. As stated previously, a function *f(t)* can be represented by an infinite Fourier series

$$f(t) = \sum_{n=-\infty}^{\infty} c_n e^{jn\omega_0 t}.$$

Taking the time derivative of both sides of this expression yields

$$\frac{df(t)}{dt} = \sum_{n=-\infty}^{\infty} (jn\omega_o) c_n e^{jn\omega_o t}.$$

From this it is seen that the i^{th} derivative with respect to time is given by

$$\frac{d^{(i)} f(t)}{dt^{(i)}} = \sum_{n=-\infty}^{\infty} (jn\omega_o)^i c_n e^{jn\omega_o t}$$

Thus it is seen that the expansion coefficient associated with the i^{th} derivative ($c^{(i)}$) is related to c_n by

$$c_n^{(i)} = c_n (jn\omega_o)^i.$$

- **Fourier coefficients of a rectangular pulse train**

The properties above are often employed when determining the Fourier coefficients of a particular waveform. To accomplish this the following general procedure is followed:

– A waveform is repeatedly differentiated until the first occurrence of an impulse function.

– If the resulting function does not consist solely of impulse functions, then the waveform is expressed as the sum of a component consisting only of impulse functions, and a remainder.

– Expansion coefficients are determined for the component of the waveform which consists of impulse functions.

– The remainder is differentiated, and the entire process repeated until only impulse functions remain.

As an example, the Fourier coefficients of a rectangular pulse train will be computed first by direct integration, and then using the properties listed above to show that the results are equivalent. A diagram of the rectangular pulse train is shown in Figure 2.

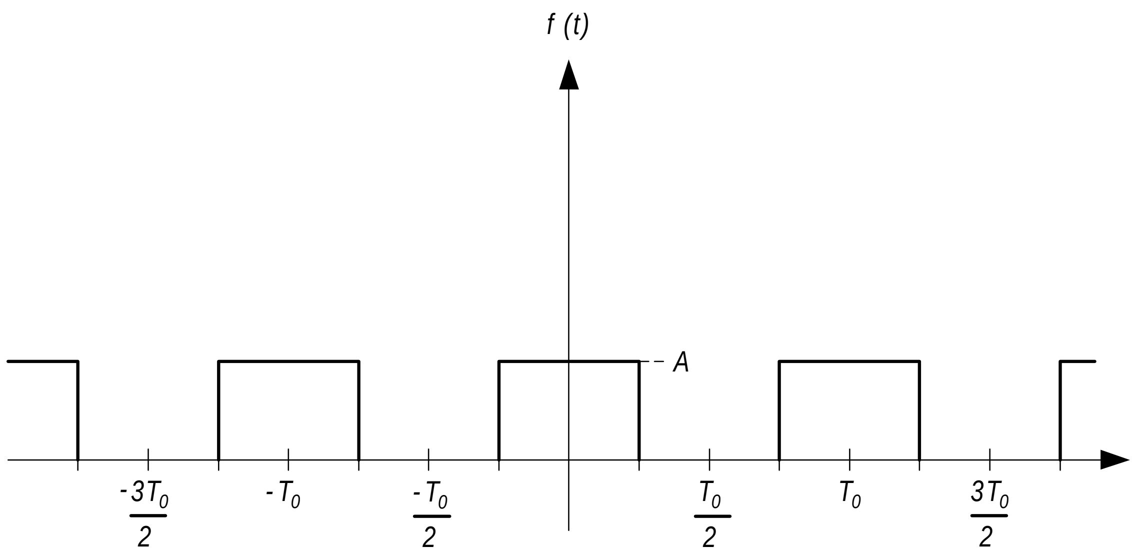

Figure 2: Rectangular Pulse Train

The Fourier coefficients associated with this pulse train are given by (for a period T_0 and arbitrary time t_1)

$$c_n = \frac{1}{T_0} \int_{t_1}^{t_1 + T_0} f(t)\, e^{-jn\omega_o t}\, dt \, .$$

Letting t_1 equal $-T_0 / 2$, c_n becomes

$$c_n = \frac{1}{T_0} \int_{-T_0/2}^{T_0/2} f(t)\, e^{-jn\omega_o t}\, dt \, .$$

The rectangular waveform effectively truncates the limits of integration, thus

$$c_n = \frac{1}{T_0} \int_{-T_0/4}^{T_0/4} A\, e^{-jn\omega_o t}\, dt$$

$$= \frac{A}{T_0} \left[\frac{e^{-jn\omega_o t}}{-jn\omega_o} \right]_{-T_0/4}^{T_0/4} .$$

Substitution of the limits of integration gives

$$c_n = \frac{A}{T_0} \frac{1}{-jn\omega_o} \left[e^{-jn\omega_o T_0/4} - e^{jn\omega_o T_0/4} \right]$$

or

$$c_n = \frac{A}{T_0} \frac{1}{jn\omega_o} \left[e^{jn\omega_o T_0/4} - e^{-jn\omega_o T_0/4} \right].$$

As stated earlier, angular frequency is

$$\omega_0 = \frac{2\pi}{T_0}$$

or

$$\omega_o T_0 = 2\pi .$$

Substituting this into the expression for c_n gives

$$c_n = \frac{A}{jn2\pi} \left[e^{jn\pi/2} - e^{-jn\pi/2} \right]$$

$$= \frac{A}{n\pi} \left[\frac{e^{jn\pi/2} - e^{-jn\pi/2}}{2j} \right].$$

But

$$\sin x = \frac{e^{jx} - e^{-jx}}{2j}$$

therefore

$$c_n = \frac{A}{n\pi}\sin(n\pi/2)$$

$$= \frac{A}{2}\frac{\sin(n\pi/2)}{n\pi/2}.$$

Finally

$$c_n = \frac{A}{2}\operatorname{sinc}(n\pi/2)$$

where

$$\operatorname{sinc}(x) = \frac{\sin x}{x}.$$

The coefficients c_n will now be found by computing $c_n^{(1)}$, the Fourier coefficients for $df(x)/dx$. A diagram of $df(x)/dx$ is shown in Figure 3. The Fourier coefficient $c_n^{(1)}$ is

$$c_n^{(1)} = \frac{1}{T_0}\int_{-T_0/2}^{T_0/2}\frac{df(t)}{dt}e^{-jn\omega_o t}\,dt.$$

Using the property

$$c_n = \frac{c_n^{(1)}}{jn\omega_o}$$

it is seen that

$$c_n = \frac{1}{jn\omega_o T_0}\int_{-T_0/2}^{T_0/2}\frac{df(t)}{dt}e^{-jn\omega_o t}\,dt.$$

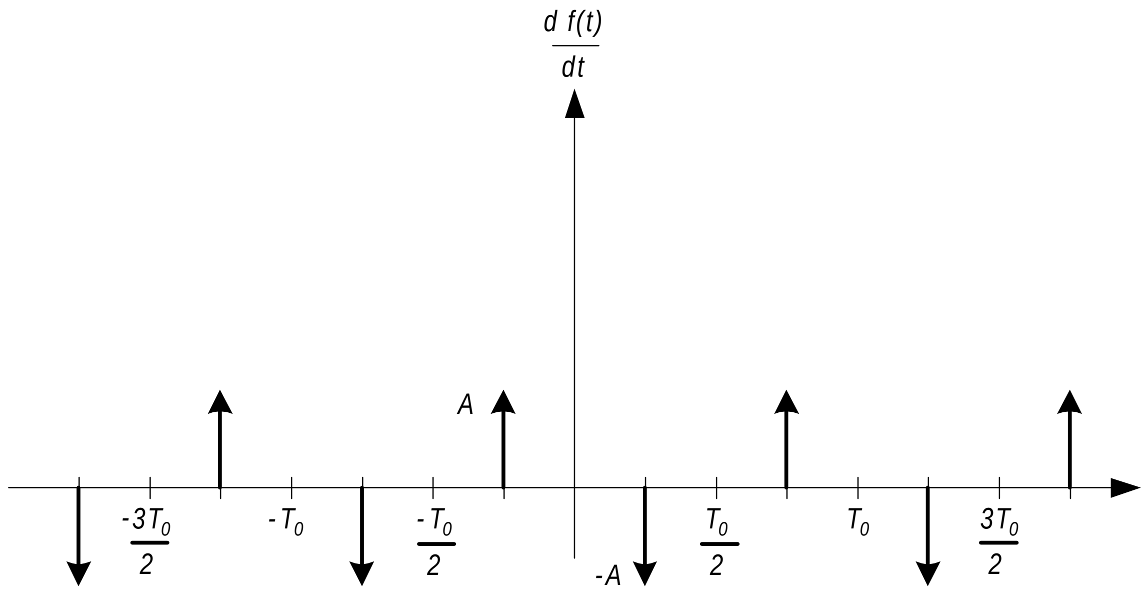

Figure 3: The Derivative of the Rectangular Pulse Train

Substituting $T_0 \omega_o = 2\pi$, and the values representing the derivative of the waveform $df(t)/dt$ into the expression above gives

$$c_n = \frac{1}{jn2\pi} \int_{-T_0/2}^{T_0/2} \left[A\,\delta(t+T_0/4) - A\,\delta(t-T_0/4) \right] e^{-jn\omega_0 t}\, dt.$$

This leads to

$$c_n = \frac{A}{jn2\pi} \left[e^{jn\omega_0 T_0/4} - e^{-jn\omega_0 T_0/4} \right]$$

$$= \frac{A}{n\pi} \left[\frac{e^{jn\pi/2} - e^{-jn\pi/2}}{2j} \right]$$

$$= \frac{A}{n\pi} \sin\left(n\frac{\pi}{2} \right)$$

$$= \frac{A}{2} \operatorname{sinc}\left(n\frac{\pi}{2} \right).$$

This is the same result that was obtained through direct integration. :-)

3.3 Trapezoidal waveforms

Digital clock signals are an extremely important group of waveforms that need to be studied. Clock signals are often approximated as square waves, however this is not very accurate. All real digital clock waveforms have a certain non-zero rise time, and a non-zero fall time. A better approximation of a digital pulse train is a trapezoidal waveform, as shown in Figure 4.

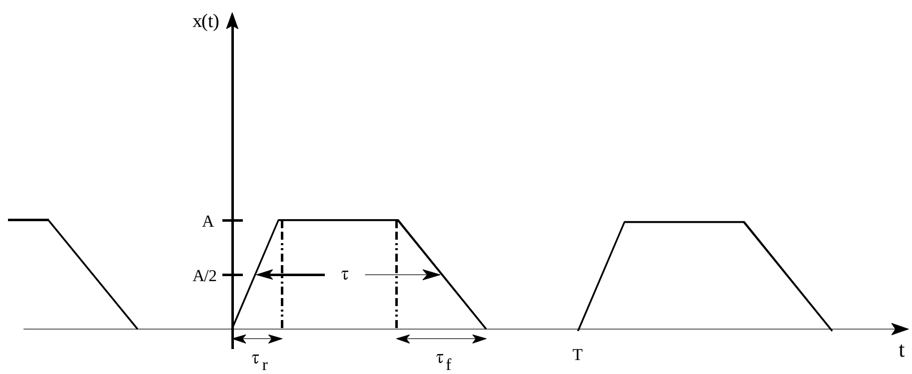

Figure 4: Approximation of a digital clock signal.

As with the waveforms examined previously, the fundamental angular frequency ω_0 of the trapezoidal pulse train is given by

$$\omega_o = 2\pi f_0 = \frac{2\pi}{T_0}.$$

It will be seen that rise time τ_r and fall time τ_f greatly affect the spectrum of a waveform. The rise time of a pulse train is defined to be the length of time needed for the signal to transition from 0 to A, where A is the amplitude of the signal. The fall time is then the length of time needed for the signal to transition from A to 0. The pulse width τ is the time needed for the signal to transition from $0.5A$ on the rising part of the signal to $0.5A$ on the falling part of the signal.

- **Fourier series of a trapezoidal waveform**

The spectrum of a trapezoidal waveform will be determined to demonstrate the effects of various rise times, and duty cycles. To accomplish this, the waveform shown above is first expanded in a Fourier series. The expansion coefficients are given by

$$c_n = \frac{1}{T} \int_{t_0}^{t_0+T} f(t)\, e^{-jn\omega_o t} dt\,.$$

Due to the nature of the waveform, two derivatives with respect to time are required to produce a train of impulse functions

$$c_n^{(2)} = \frac{1}{T} \int_{t_0}^{t_0+T} \frac{d^2 f(t)}{dt^2} e^{-jn\omega_o t} dt\,.$$

which becomes

$$c_n^{(2)} = \frac{1}{T} \Bigg\{ \int_{0^-}^{0^+} \frac{A}{\tau_r} \delta(t)\, e^{-jn\omega_o t} dt + \int_{\tau_1^-}^{\tau_1^+} -\frac{A}{\tau_r} \delta(t-\tau_1) e^{-jn\omega_o t} dt$$

$$+ \int_{\tau_2^-}^{\tau_2^+} -\frac{A}{\tau_f} \delta(t-\tau_2) e^{-jn\omega_o t} dt + \int_{\tau_3^-}^{\tau_3^+} \frac{A}{\tau_f} \delta(t-\tau_3) e^{-jn\omega_o t} dt \Bigg\}$$

where

$$\tau_1 = \tau_r$$

$$\tau_2 = \tau + \frac{\tau_r - \tau_f}{2}$$

and

$$\tau_3 = \tau + \frac{\tau_r + \tau_f}{2}\,.$$

Performing the various integrations gives

$$c_n^{(2)} = \frac{A}{T}\left\{\frac{1}{\tau_r}e^{0} - \frac{1}{\tau_r}e^{-jn\omega_o\tau_1} - \frac{1}{\tau_f}e^{-jn\omega_o\tau_2} + \frac{1}{\tau_f}e^{-jn\omega_o\tau_3}\right\}$$

and substitution of the expressions for τ_1, τ_2, and τ_3 given above yields

$$c_n^{(2)} = \frac{A}{T}\left\{\frac{1}{\tau_r} - \frac{1}{\tau_r}e^{-jn\omega_o\tau_r} - \frac{1}{\tau_f}e^{-jn\omega_o\left(\tau + \frac{\tau_r - \tau_f}{2}\right)} + \frac{1}{\tau_f}e^{-jn\omega_o\left(\tau + \frac{\tau_r + \tau_f}{2}\right)}\right\}.$$

If the rise time of the clock signal is equal to its fall time, which is often a good approximation, this expression can be simplified. Let

$$\tau_r = \tau_f$$

and then

$$c_n^{(2)} = \frac{A}{T}\frac{1}{\tau_r}\left\{1 - e^{-jn\omega_o\tau_r} - e^{-jn\omega_o\tau} + e^{-jn\omega_o(\tau + \tau_r)}\right\}.$$

Factoring out

$$e^{-jn\omega_o\frac{\tau + \tau_r}{2}}$$

and grouping terms gives

$$c_n^{(2)} = \frac{A}{T}\frac{1}{\tau_r}e^{-jn\omega_o\frac{\tau + \tau_r}{2}}\left\{e^{jn\omega_o\frac{\tau}{2}}\left(e^{jn\omega_o\frac{\tau_r}{2}} - e^{-jn\omega_o\frac{\tau_r}{2}}\right) - e^{-jn\omega_o\frac{\tau}{2}}\left(e^{jn\omega_o\frac{\tau_r}{2}} - e^{-jn\omega_o\frac{\tau_r}{2}}\right)\right\}.$$

Now

$$\sin\left(n\omega_o\frac{\tau_r}{2}\right) = \frac{e^{jn\omega_o\frac{\tau_r}{2}} - e^{-jn\omega_o\frac{\tau_r}{2}}}{2j}$$

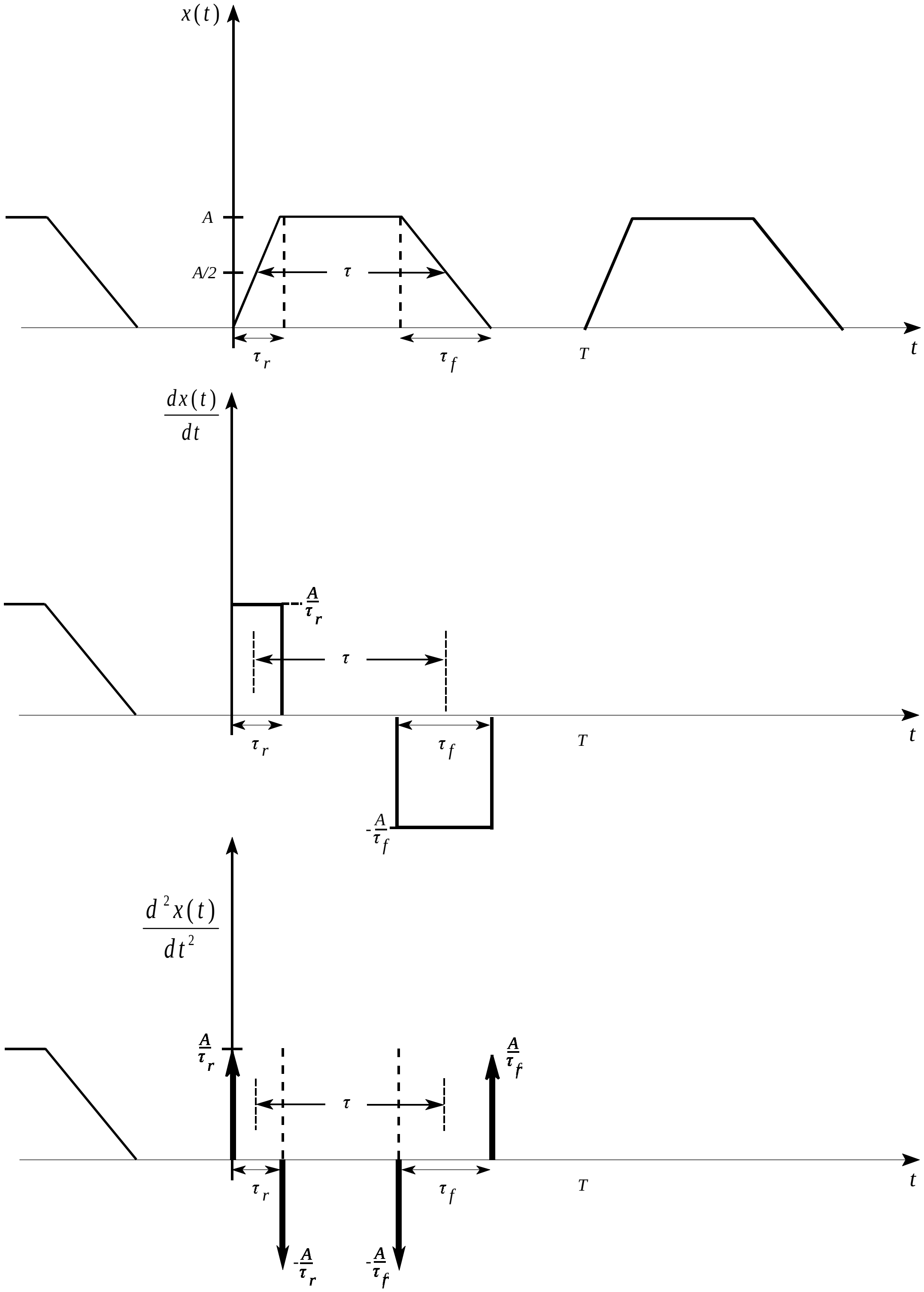

Figure 5: Diagram of the Trapezoidal Waveform and Its Derivatives

therefore

$$c_n^{(2)} = 2j\frac{A}{T}\frac{1}{\tau_r}\, e^{-jn\omega_o\frac{\tau+\tau_r}{2}}\ \sin\left(n\omega_o\frac{\tau_r}{2}\right)\left(e^{jn\omega_o\frac{\tau}{2}} - e^{-jn\omega_o\frac{\tau}{2}}\right)$$

and

$$c_n^{(2)} = -4\,\frac{A}{T}\,\frac{1}{\tau_r}\, e^{-jn\omega_o\frac{\tau+\tau_r}{2}}\ \sin\left(n\omega_o\,\frac{\tau_r}{2}\right)\,\sin\left(n\omega_o\,\frac{\tau}{2}\right)\ .$$

Applying the property

$$c_n^{(2)} = c_n\,(\,jn\omega_o)^2$$

gives

$$c_n = \frac{4}{n^2\omega_o^2}\,\frac{A}{T}\,\frac{1}{\tau_r}\, e^{-jn\omega_o\frac{\tau+\tau_r}{2}}\ \sin\left(n\omega_o\,\frac{\tau_r}{2}\right)\,\sin\left(n\omega_o\,\frac{\tau}{2}\right).$$

This may be expressed as

$$c_n = A\,\frac{\tau}{T}\;\frac{\sin\left(n\omega_o\,\frac{\tau}{2}\right)}{\frac{1}{2}n\omega_o\tau}\;\frac{\sin\left(n\omega_o\,\frac{\tau_r}{2}\right)}{\frac{1}{2}n\omega_o\tau_r}\; e^{-jn\omega_o\frac{\tau+\tau_r}{2}}$$

or

$$c_n = A\,\frac{\tau}{T}\ \mathrm{sinc}\left(n\,\omega_o\,\frac{\tau}{2}\right)\ \mathrm{sinc}\left(n\,\omega_o\,\frac{\tau_r}{2}\right)\ e^{-jn\omega_o\frac{\tau+\tau_r}{2}}\ .$$

It must be remembered that this expression for c_n is only valid for the special case of $\tau_r = \tau_f$.

- **magnitude spectrum envelope**

The amplitudes of the expansion coefficients determined for a particular waveform fall within a certain envelope. For the trapezoidal waveform examined above, this envelope is given by

$$env_{trap.} = \text{upper bound of:} \quad 2A\frac{\tau}{T}\left|\text{sinc}(\pi\tau f)\right| \left|\text{sinc}(\pi\tau_r f)\right|$$

where $f = n/T$. In order to quickly deduce the significance that high frequency spectral components associated with a waveform such as this may have, upper bounds can be established on this envelope. These upper bounds represent "worst case", or maximum possible expansion coefficient amplitudes for a given frequency range.

The spectral bounds are established by first taking the logarithm of both sides of the waveform envelope expression

$$20\log_{10}(env_{trap.}) = 20\log_{10}\left(2A\frac{\tau}{T}\right) + 20\log_{10}\left|\text{sinc}(\pi\tau f)\right| + 20\log_{10}\left|\text{sinc}(\pi\tau_r f)\right|.$$

It is seen that the first term

$$20\log_{10}\left(2A\frac{\tau}{T}\right)$$

has a slope of 0 dB per decade, and a level of $2A\tau/T = 2A\tau f_o$. The second term and third terms have the form $\sin x/x$. For small arguments $\sin x \cong x$, therefore

$$\left|\frac{\sin x}{x}\right| \leq \begin{cases} 1 & \text{... for small } x \\ \dfrac{1}{|x|} & \text{... for large } x \end{cases}$$

which can be drawn as two linear asymptotes, the first with a slope of 0 dB/decade, and the second with a slope of -20 dB/decade.

Thus, the term $20\log_{10}\left|\text{sinc}(\pi\tau f)\right|$, has an asymptote with a slope of 0 dB/decade and an asymptote with a slope of -20 dB/decade. These asymptotes meet at $f = 1/\pi\tau$. The third term, $20\log_{10}\left|\text{sinc}(\pi\tau_r f)\right|$, also has an asymptote with a slope of 0 dB/decade and an asymptote with a slope of -20 dB per decade, which meet at $f = 1/\pi\tau_r$. The spectral bounds of the trapezoidal waveform therefore consist of a three segment line with two breakpoints. The first segment has a slope of 0 dB/decade. The second segment, starting at $f = 1/\pi\tau$, has a slope of -20 dB/decade. The third segment, starting at $f = 1/\pi\tau_r$, has a slope of -40 dB/decade.

If the duty cycle is short enough that the frequency $1/(\pi\tau)$ is greater than the fundamental frequency,

$$\frac{1}{\pi\tau} > \frac{2\pi}{T} \qquad (\tau < \frac{T}{2}),$$

then the spectrum's envelope will have a slope of 0 dB per decade from the fundamental to that frequency. If the frequency $1/(\pi\tau)$ occurs before the fundamental frequency, then the envelope begins with a slope of -20 dB per decade. The envelope then begins a much sharper descent of -40 dB per decade at $f = 1/\pi\tau_r$.

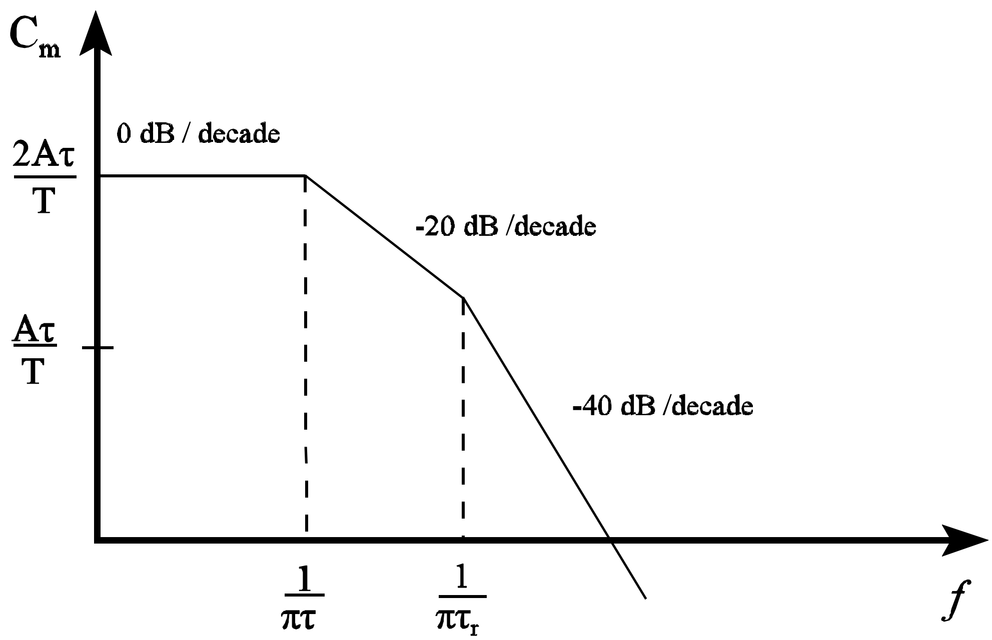

Figure 6: Spectral Bounds on the Trapezoidal Waveform (Paul; p. 365)

- **comparison of trapezoidal waveform spectra**

– **relationship between risetime and signal spectrum**

In Figure 7, the magnitude spectra of two trapezoidal waveforms with different risetimes are plotted as a function of frequency. The risetime of waveform 1 is 0.1 ns and the risetime of waveform 2 is 0.5 ns. Both waveforms have 5V amplitudes, with expansion coefficient magnitudes plotted in dBμV. The fundamental frequencies of both waveforms are 100 MHz, and the duty cycle for both waveforms is 50% $(\tau = 0.5T)$.

As shown above, the envelope of the magnitude spectrum has a slope of 0 dB per decade until it reaches the frequency

$$\frac{1}{\pi\tau} = \frac{1}{\pi\left(.5\times1/(100\,MHz)\right)} = 63.66\,MHz \qquad .$$

This frequency, however, is lower than the fundamental frequency itself. Therefore, the envelopes are plotted beginning with a slope of -20 dB per decade at the fundamental frequency of 100 MHz. Both envelopes decrease at a rate of -20 dB per decade until

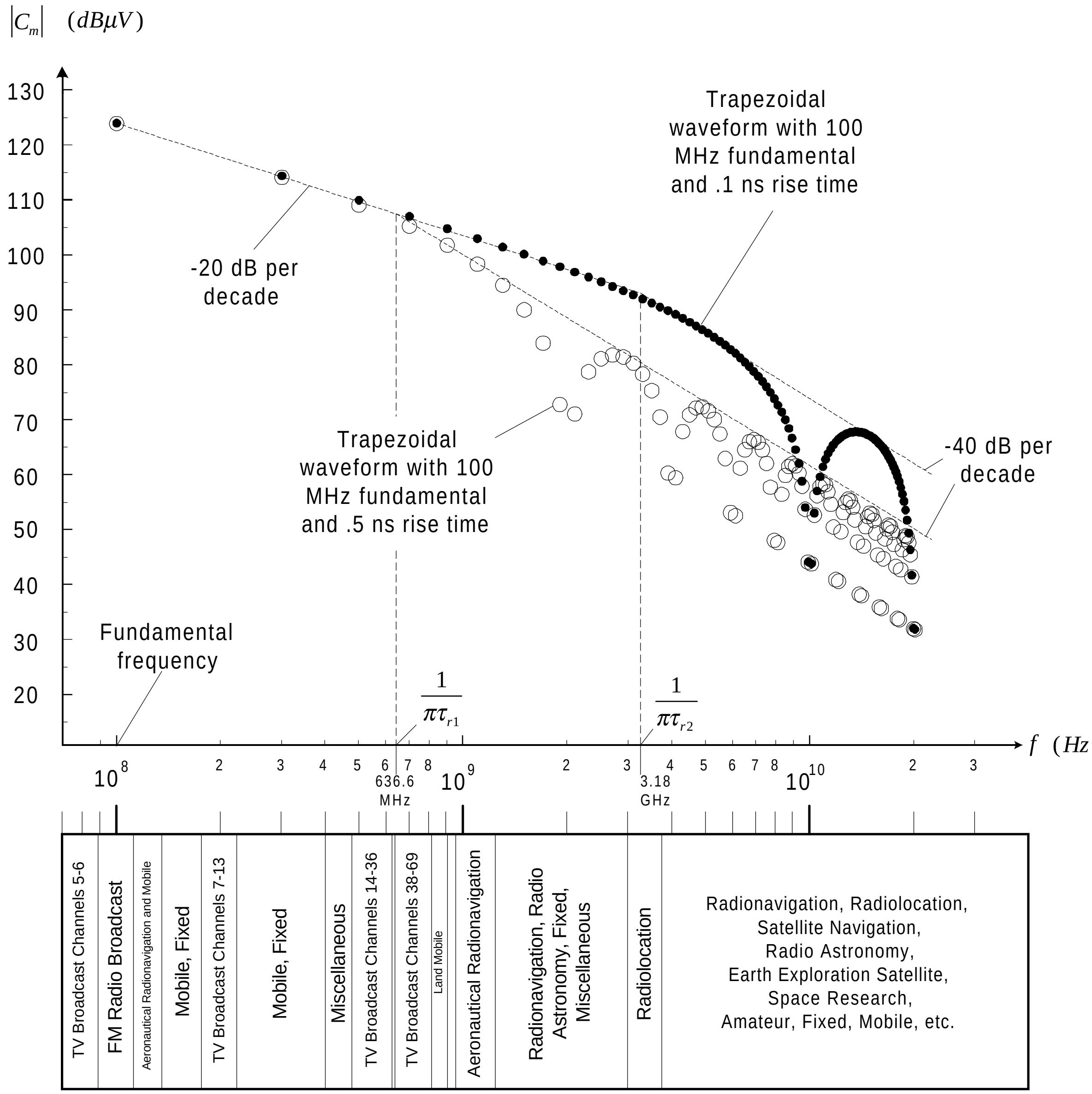

Figure 7: Magnitude spectra of trapezoidal waveforms with different rise times

envelope 2 reaches its second corner frequency at

$$\frac{1}{\pi\tau_{r_2}} = \frac{1}{\pi\,(.5\times10^{-9})} = 636.6 MHz\,.$$

After this, envelope 2 decreases at a rate of -40 dB per decade while envelope 1 continues to decrease at -20 dB per decade. The second corner frequency for envelope 1 occurs at

$$\frac{1}{\pi\tau_{r_1}} = \frac{1}{\pi\,(.1\times10^{-9})} = 3.183 GHz\,.$$

At this point, envelope 1 begins to decrease at -40 dB per decade. Above this frequency, notice that envelope 1 is about 13 dBµV higher than envelope 2.

It is seen in this figure that the energy of a signal such as the trapezoidal clock waveform is spread over a broad range of frequencies, and that the high frequency content of such a waveform is impacted significantly by the rise time of the signal.

– **relationship between duty cycle and signal spectrum**

Now trapezoidal waveform with various duty cycles will be compared. In Figure 8, the spectra of two trapezoidal waveforms is plotted as a function of frequency. Waveform 1 has a duty cycle of 50%, while waveform 2 has a duty cycle of 25%. All other quantities of the waveforms are the same (fundamental frequency is 10 MHz, rise time is 1 ns, and the amplitude is 5 V). As with the previous example, since the corner frequency for envelope 1

$$\frac{1}{\pi\tau_1} = \frac{1}{\pi\left(.5\times1/(10 MHz)\right)} = 6.366 MHz$$

is below the fundamental frequency, the plot of envelope 1 begins at the fundamental frequency and decreases at -20 dB/decade. The first corner frequency for envelope 2 occurs at

$$\frac{1}{\pi\tau_2} = \frac{1}{\pi\left(.25\times1/(10 MHz)\right)} = 12.73 MHz\,.$$

This frequency is above the 10 MHz fundamental frequency. Envelope 2 will then have a slope of 0 dB per decade until it reaches 12.73 MHz, where it will begin to decrease at -20 dB per decade. Since 12.73 MHz is so close to the fundamental, the effect of the 0 dB per decade portion is difficult to detect.

The second corner frequency for both envelopes occurs at

$$\frac{1}{\pi\tau_r} = \frac{1}{\pi\,(1\times10^{-9})} = 318.3MHz\ .$$

This frequency is the same for both waveforms because they have the same rise time. Both envelopes begin to decrease at 40 dB per decade at this point.

Notice that although the shapes of both spectra are similar, envelope 1 is about 3 dB higher than envelope 2 over the entire range of frequencies. This is the expected result because the 25% duty cycle waveform should carry about half of the energy (-3 dB) that the 50% duty cycle waveform carries.

The important observation here is that the high-frequency content of the signals examined was affected significantly by changing the risetime of the waveform. The length of the waveform duty cycle had almost no effect on the high frequency components. Only a 3 dB decrease of the magnitudes of all spectral components occurred, and this is because the overall energy of the 25% duty cycle waveform is half that of the 50% duty cycle waveform.

The spectra of additional waveforms is shown in Figure 9. This figure shows the spectra of trapezoidal waveforms with three different duty cycles (50%, 65%, and 10%). All other quantities for the signals are identical (fundamental frequency is 100 MHz, rise time is 0.2 ns, and the amplitude is 5 V). Let the magnitude spectra of the 50%, 65%, 10% duty cycle waveforms be described by envelope 1, envelope 2 and envelope 3, respectively.

The first corner frequency for envelope 1 (upper left hand corner) occurs at

$$\frac{1}{\pi\tau_1} = \frac{1}{\pi\left(.5\times1/(100MHz)\right)} = 63.66MHz\ .$$

This is below the fundamental frequency of the waveform, so envelope 1 begins to decrease at a rate of -20 dB/decade. The second corner frequency of envelope 1 occurs at

$$\frac{1}{\pi\tau_r} = \frac{1}{\pi\,(.2\ ns)} = 1.592GHz\ \ .$$

This frequency is the same for all three spectra, since the waveforms all have the same rise time. Envelope 1 begins to decrease at -40 dB/ decade above this frequency.

The spectrum of the 65% duty cycle waveform is shown in the upper right hand corner of the figure. The first corner frequency for the envelope of this spectrum (envelope 2) occurs at

$$\frac{1}{\pi\tau_2} = \frac{1}{\pi\left(.65\times1/(100MHz)\right)} = 48.97MHz\quad .$$

This is also below the fundamental frequency, so envelope 2 also is plotted with an initial slope of -20 dB per decade. The second corner frequency for envelope 2 occurs at 1.592 GHz, which was the same frequency for envelope 1. Therefore, the envelopes of the magnitude spectra for waveforms having 50% and 65% duty cycles are the same. The

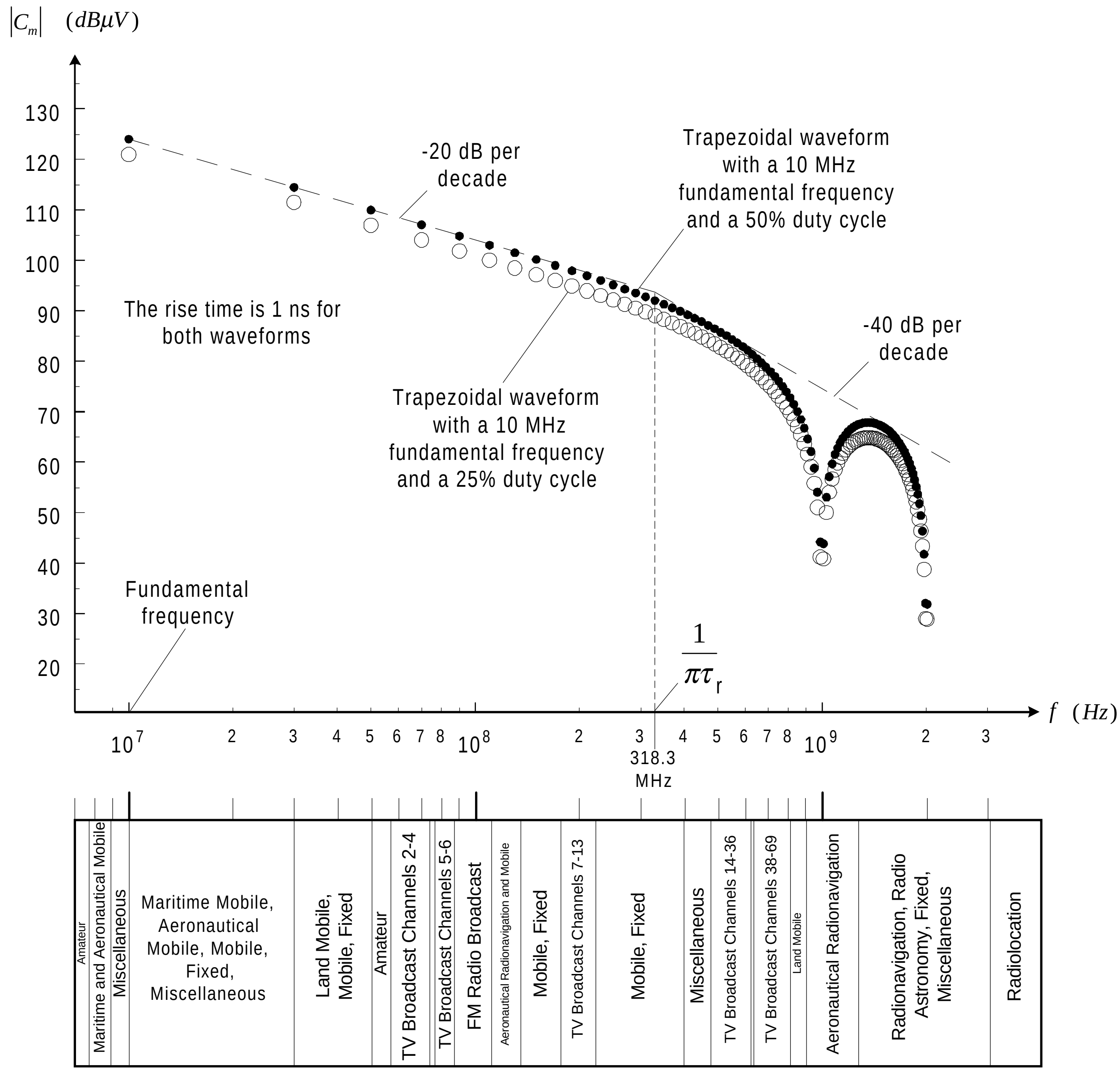

Figure 8: Magnitude spectra of a 50% and a 25% duty cycle trapezoidal waveform

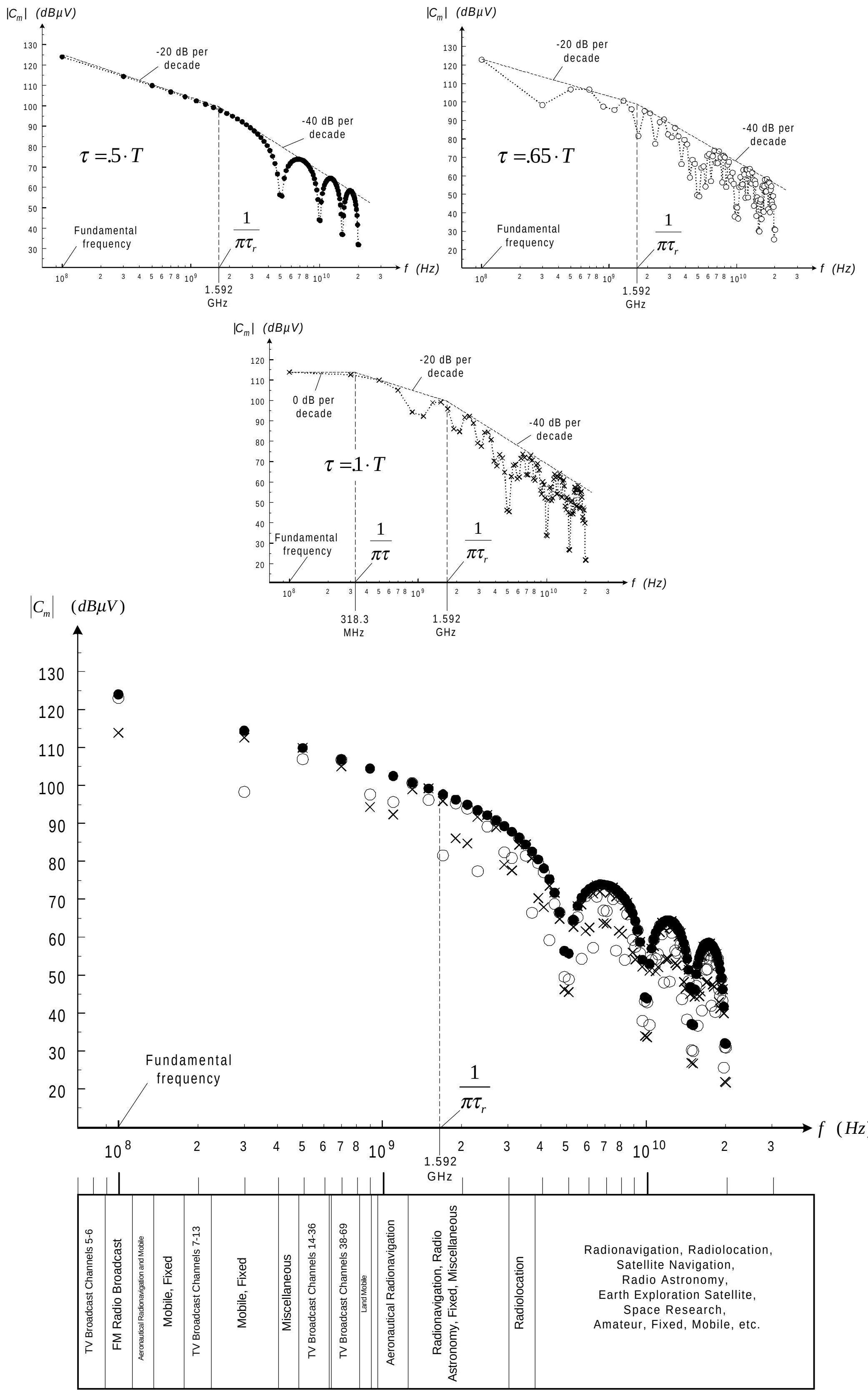

Figure 9: Spectra of Trapezoidal Signals with Random Duty Cycles

individual spectral components are different, but the bounds on the magnitude spectra take the same shape and amplitude.

Now the spectral envelope of the 10% duty cycle waveform will be examined. (This spectrum can be found in the middle of the figure). The first corner frequency for envelope 3 is

$$\frac{1}{\pi\tau_3} = \frac{1}{\pi\left(.1\times 1/(100\,MHz)\right)} = 318.3\,MHz\,.$$

Therefore, this envelope has a slope of 0 dB/decade from the fundamental frequency until it reaches about 318 MHz. Then it decreases at -20 dB/decade. Like the other two envelopes, envelope 3 decreased at -40 dB/decade after 1.592 GHz.

Notice that although the individual spectral components of the various waveforms are different at most frequencies, the envelopes are nearly identical for the high frequency portion of the spectrum. Thus, duty cycle does not play as important a role in determining the high frequency components of a trapezoidal waveform as does the rise time of the signal.

3.4 Fourier Transforms and Non-Periodic Waveforms

Just as a periodic waveform can be represented by an equivalent series (Fourier series), an aperiodic waveform can be expressed by an equivalent representation known as the *inverse Fourier Transform*. Let $f_p(t)$ represent a periodic function

$$f_p(t) = \sum_{m=-\infty}^{\infty} c_n e^{jn\omega_o t} \quad .$$

This can be rewritten as

$$f_p(t) = \sum_{n=-\infty}^{\infty} T_0\, c_n e^{jn\omega_o t}\, \frac{1}{T_0} \quad .$$

By using $T_0 = \frac{2\pi}{\omega_o}$, this becomes

$$f_p(t) = \frac{1}{2\pi} \sum_{n=-\infty}^{\infty} T_0\, c_n e^{jn\omega_o t}\, \omega_o\,.$$

If T_0 the period of $f_p(t)$ is extended to infinity, the resulting aperiodic function can be represented by

$$\lim_{T_0 \to \infty} f_p(t) = f(t) = \frac{1}{2\pi} \lim_{T_0 \to \infty} \left\{ \sum_{n=-\infty}^{\infty} T_0 c_n e^{jn\omega_o t} \omega_o \right\}.$$

The term $T_0 c_n$ can be written as

$$T_0 c_n = T_0 \cdot \frac{1}{T_0} \int_{-T_0/2}^{T_0/2} f_p(t) e^{-jn\omega_o t} dt = \int_{-T_0/2}^{T_0/2} f_p(t) e^{-jn\omega_o t} dt.$$

As T_0 approaches infinity, $f_p(t)$ approaches $f(t)$ and $n\omega_o$ becomes a new variable ω

$$\lim_{T_0 \to \infty} T_0 c_n = \int_{-\infty}^{\infty} f(t) e^{-j\omega t} dt = \int_{-\infty}^{\infty} f(\zeta) e^{-j\omega\zeta} d\zeta.$$

Recalling that

$$\lim_{T_0 \to \infty} f_p(t) = f(t) = \frac{1}{2\pi} \lim_{T_0 \to \infty} \left\{ \sum_{n=-\infty}^{\infty} T_0 c_n e^{jn\omega_o t} \omega_o \right\},$$

and applying the new variable ω, the function $f(t)$ becomes

$$f(t) = \frac{1}{2\pi} \lim_{T_0 \to \infty} \left\{ \sum_{n=-\infty}^{\infty} T_0 c_n e^{j\omega t} \Delta\omega \right\}$$

where $\Delta\omega = \omega_0$. The infinite sum now becomes an integral from $(-\infty, \infty)$ over the variable ω. Using the representation derived above for $\lim_{T_0 \to \infty} T_0 c_n$, $f(t)$, can now be written as

$$f(t) = \frac{1}{2\pi} \int_{-\infty}^{\infty} \left\{ \int_{-\infty}^{\infty} f(\zeta) e^{-j\omega\zeta} d\zeta \right\} e^{j\omega t} d\omega \ .$$

Let

$$F(\omega) = \int_{-\infty}^{\infty} f(\zeta) e^{-j\omega\zeta} d\zeta.$$

$F(\omega)$ known is the *Fourier transform* of $f(\zeta)$. Now $f(t)$ can be expressed

$$f(t) = \frac{1}{2\pi} \int_{-\infty}^{\infty} F(\omega)\, e^{j\omega t}\, d\omega$$

where the function $f(t)$ is the *inverse Fourier transform* of $F(\omega)$.

This result indicates that the function $f(t)$ can be represented by a continuous superposition of exponentials weighted by a function $F(\omega)$ for each frequency ω. If the frequency variable $f = \omega / 2\pi$ is to be used instead of the angular frequency variable ω, the Fourier transform pairs become

$$F(f) = \int_{-\infty}^{\infty} f(t)\, e^{-j2\pi f t}\, dt$$

and

$$f(t) = \int_{-\infty}^{\infty} F(f)\, e^{j2\pi f t}\, df.$$

- **frequency content of signals**

The Fourier transform is used to examine the frequency content of aperiodic signals. In the following example the Fourier transform will be used to examine the frequency spectrum of a short pulse (broadband signal). This pulse can be used to represent an electrostatic discharge, an electromagnetic pulse, or a lightning event. An approximation of a short pulse is a Gaussian function

$$x(t) = e^{-\pi(at)^2}$$

A plot of $x(t)$ can be found in Figure 10. The Fourier transform of $x(t)$ (using the frequency variable f) is

$$X(f) = \int_{-\infty}^{\infty} x(t)\, e^{-j2\pi f t}\, dt.$$

Using Fourier transform pairs and the scaling property, the Fourier transform of $x(t)$ is found to be

$$X(f) = \frac{1}{|a|}\, e^{\left(-\pi(f/a)^2\right)}.$$

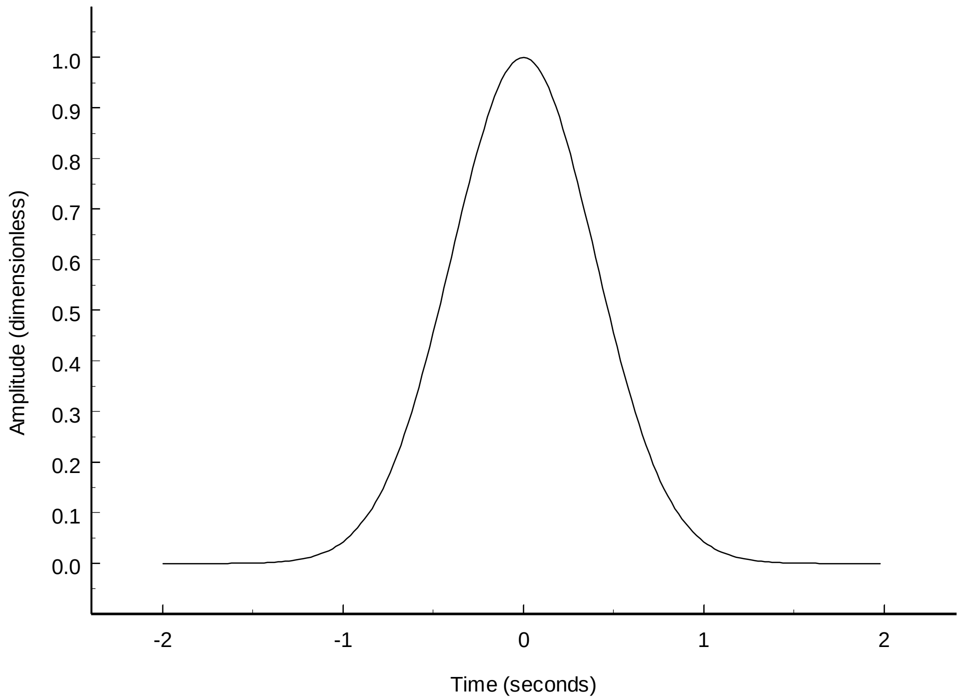

Figure 10: Amplitude of Pulse vs. Time

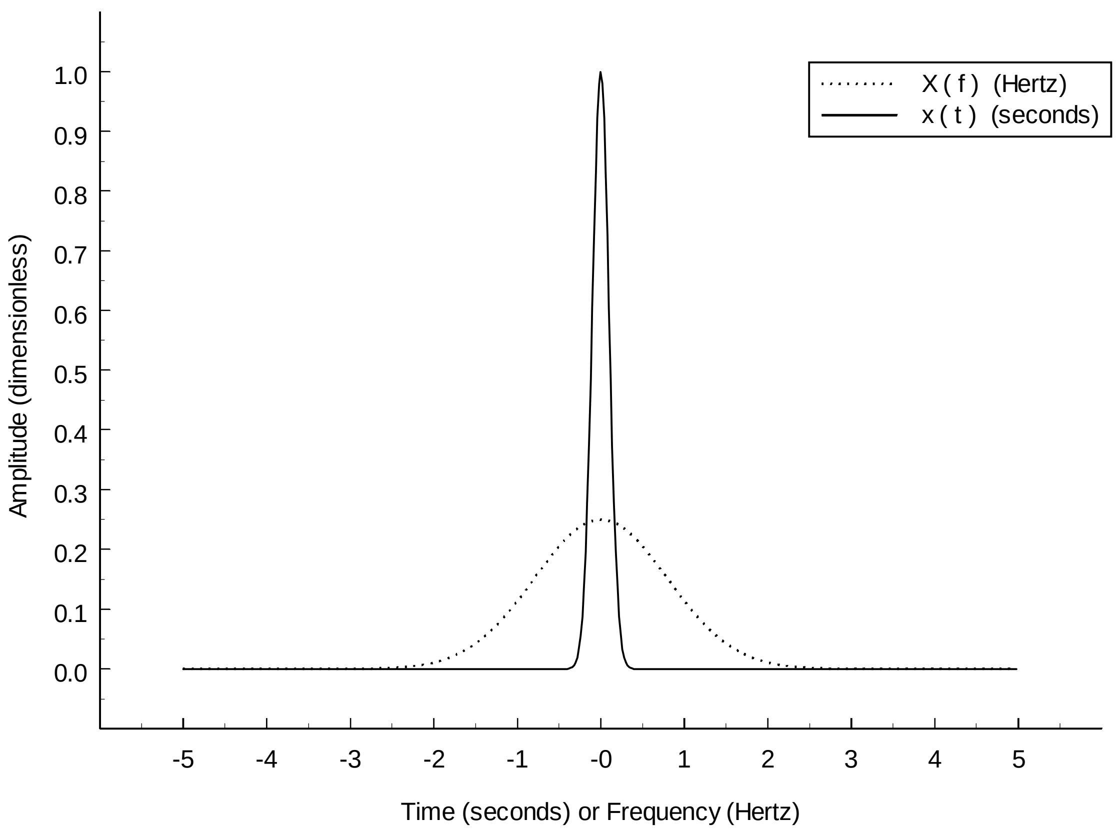

Figure 11: Illustration of the Frequency Content of a Narrow Pulse

As the parameter a increases, the frequency spectrum of $x(t)$ widens out. This effect is shown in Figure 11. In this plot, a was chosen to be 4.

This demonstrates that pulses or signals which are narrow in time have broad frequency spectra. Thus short duration pulse signals, such as an electrostatic discharge, an electromagnetic pulse, or a lightning event are typically rich in spectral content. These signals can then interfere with many electronic systems operating at a broad range of frequencies.

Another example involving the frequency content of aperiodic signals will now be presented by examining a trapezoidal pulse. A diagram of a trapezoidal pulse is shown in Figure 12. The Fourier transform of this waveform will be computed by using the first and second derivatives of x(t). Let

$$x^{/}(t) = \frac{dx(t)}{dt}$$

and

$$x^{//}(t) = \frac{d^2x(t)}{dt^2}.$$

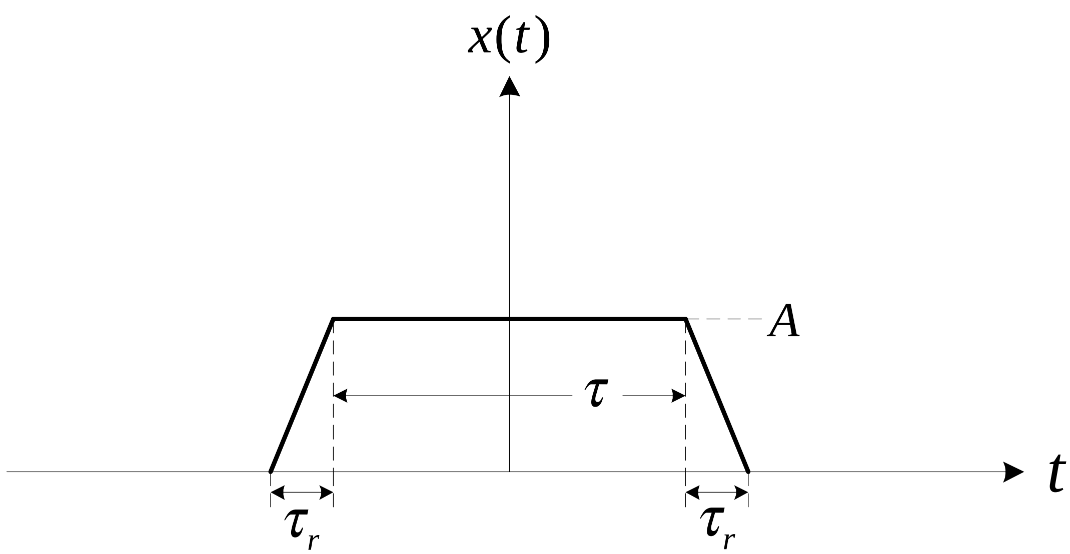

Figure 12: Aperiodic Trapezoidal Pulse

The second derivative of x(t), as shown in Figure 13, can be written as

$$x^{//}(t) = \frac{A}{\tau_r}\left[\delta\left(t+\frac{\tau}{2}+\tau_r\right) - \delta\left(t+\frac{\tau}{2}\right) - \delta(t-\tau_r) + \delta\left(t-\frac{\tau}{2}-\tau_r\right)\right]$$

Let

$$X''(\omega) = \int_{-\infty}^{\infty} x''(t)\, e^{-j\omega t}\, dt$$

and let $\tau_1 = \tau/2 + \tau_r$. Then

$$X''(\omega) = \frac{A}{\tau_r}\left[e^{j\omega\tau_1} - e^{j\omega\tau/2} - e^{-j\omega\tau/2} + e^{-j\omega\tau_1}\right]$$

$$X''(\omega) = \frac{2A}{\tau_r}\left[\cos\left[\omega\left(\frac{\tau}{2} + \tau_r\right)\right] - \cos\left(\frac{\omega\tau}{2}\right)\right].$$

Now

$$X''(\omega) = (j\omega)^2 X(\omega)$$

where

$$X(\omega) = \int_{-\infty}^{\infty} x(t)\, e^{-j\omega t}\, dt.$$

Then

$$X(\omega) = \frac{2A}{(j\omega)^2 \tau_r}\left[\cos\left[\omega\left(\frac{\tau}{2} + \tau_r\right)\right] - \cos\left(\frac{\omega\tau}{2}\right)\right]$$

and since $\omega = 2\pi f$,

$$X(f) = \frac{2A}{\tau_r (2\pi f)^2}\left[\cos\left(2\pi f \frac{\tau}{2}\right) - \cos\left(2\pi f\left(\frac{\tau}{2} + \tau_r\right)\right)\right].$$

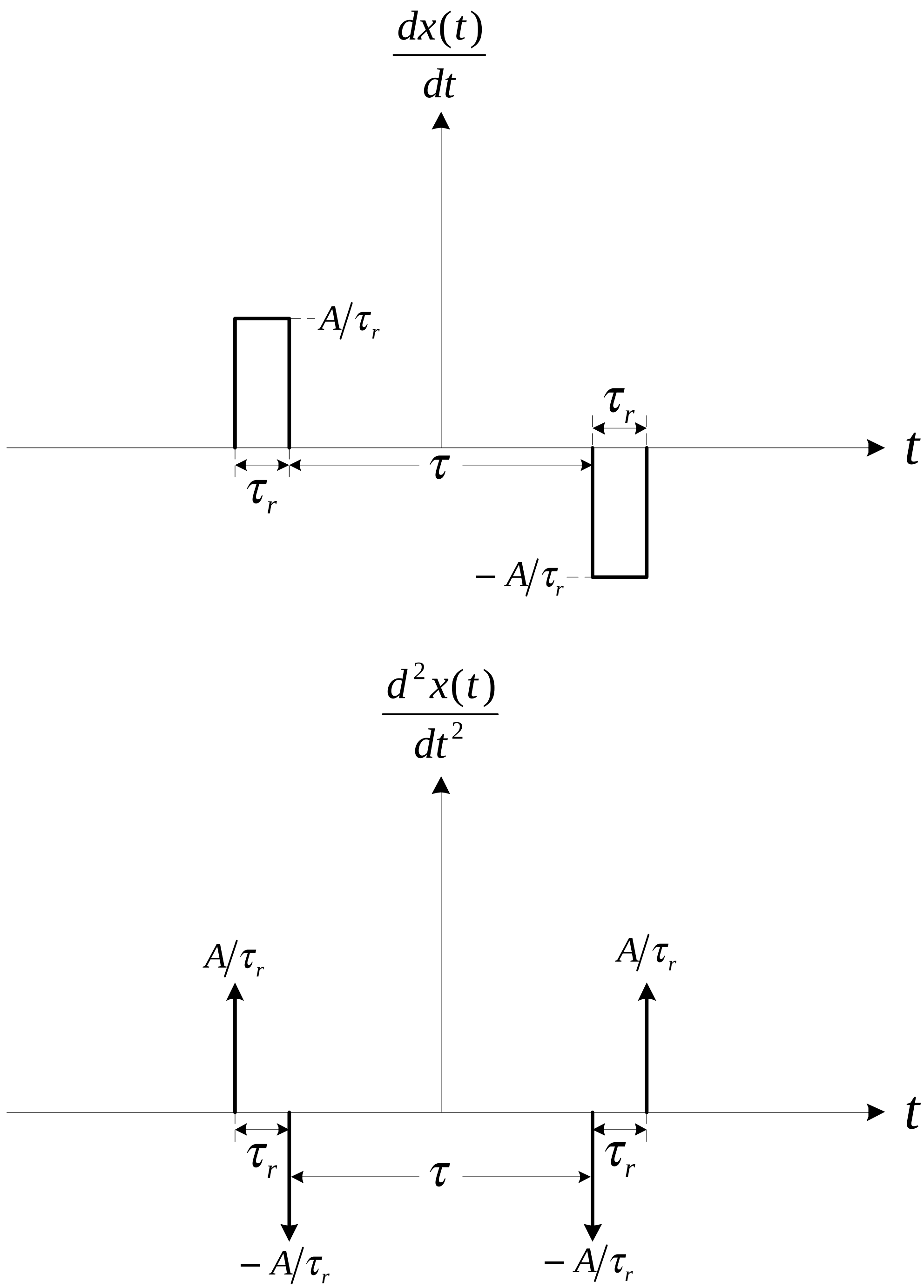

Figure 13: First and second derivatives of the trapezoidal pulse

– **relationship between rise time on pulse spectrum**

The spectra of two waveforms with the same pulse width, τ, but different rise times are shown in Figure 14 and Figure 15. Both spectral envelopes have a slope of 0 dB/decade from 0 Hz to the first corner frequency, which is the same for both waveforms. This frequency is

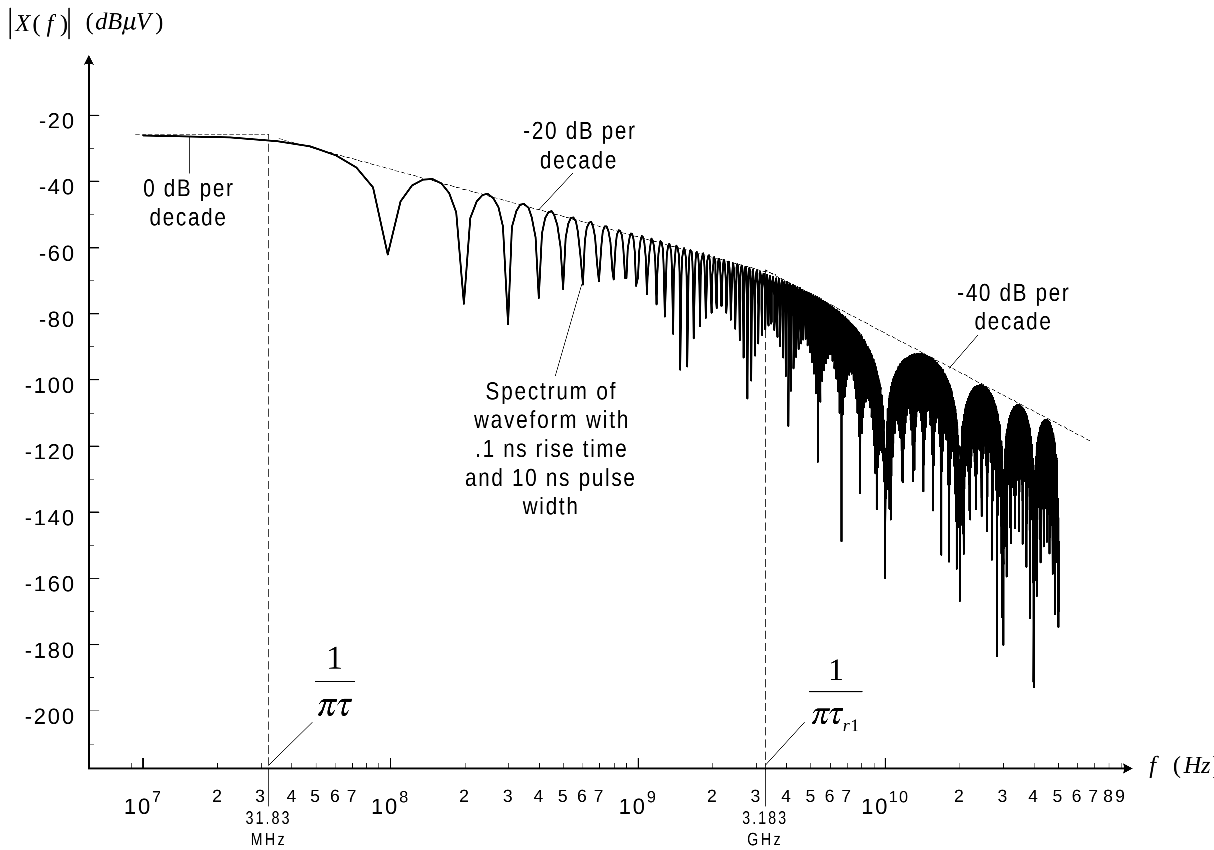

Figure 14: Magnitude spectrum of pulse with a .1 ns rise time and a 10 ns pulse width

$$\frac{1}{\pi\tau} = \frac{1}{\pi(10\,ns)} = 31.83\,MHz \ .$$

Above this frequency, both envelopes decrease at a rate of -20 dB/ decade.

The second corner frequency occurs at a lower frequency for the spectrum waveform having a 1 ns risetime (Figure 15). This second corner frequency occurs at

$$\frac{1}{\pi\tau_{r_2}} = \frac{1}{\pi(1\,ns)} = 318.3\,MHz \ .$$

Above this frequency, the spectral envelope of the waveform decreases at -40 dB/decade, while the spectral envelope of the pulse having a .1 ns risetime continues to decrease at a rate of only -20 dB/decade. At the frequency

$$\frac{1}{\pi\tau_{r_1}} = \frac{1}{\pi(.1\,ns)} = 3.183\,GHz \ ,$$

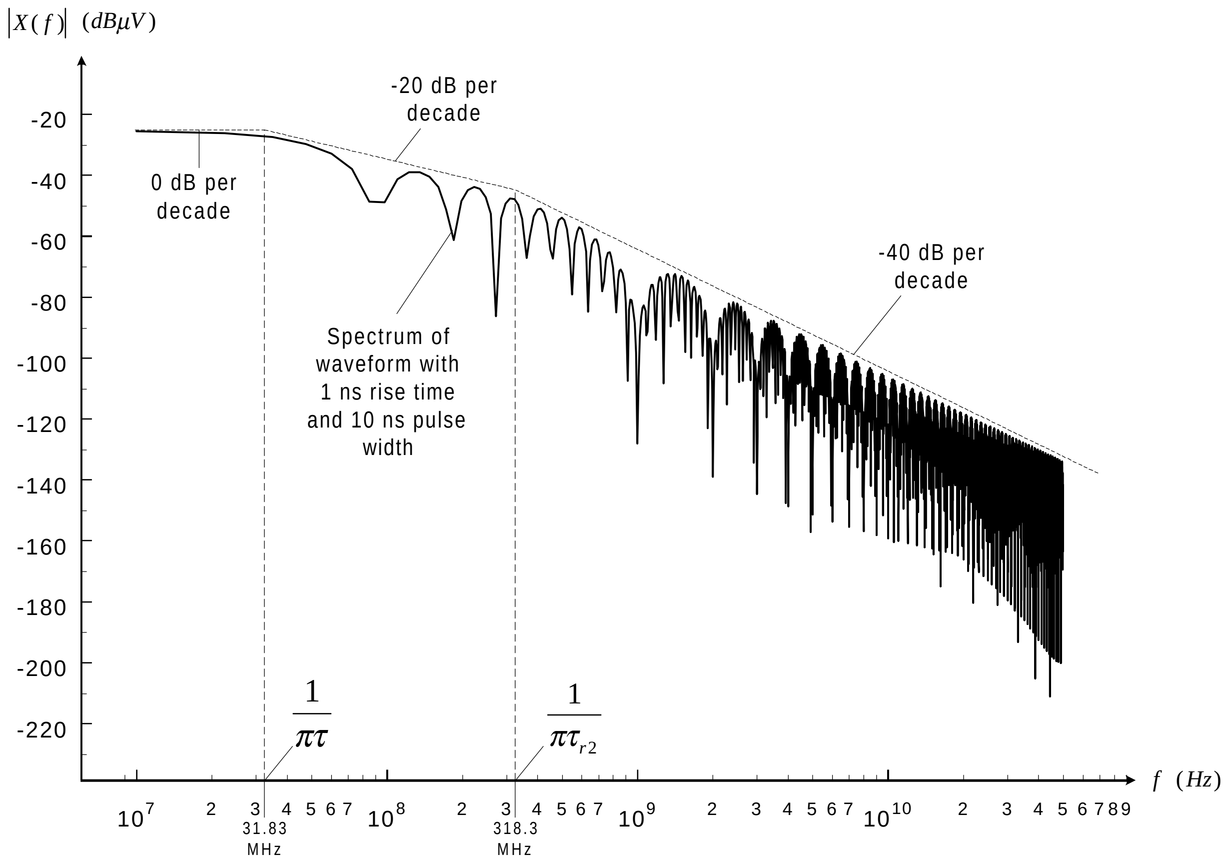

Figure 15: Magnitude spectrum of pulse with a 1 ns rise time and a 10 ns pulse width

the spectral envelope of the pulse with the .1 ns rise time begins to decrease at a rate of -40 dB/ decade.

A direct comparison of the envelopes of the spectra of these two waveforms can be seen in Figure 16 . In the frequency range above 3.183 Ghz it is noted that the spectral envelope of the waveform with a .1 ns rise time is 20 dB higher than that of the pulse with the 1 ns rise time. Thus even for an aperiodic trapezoidal pulse, the high frequency content is greatly affected by the rise time of the pulse.

– **relationship between pulse width and spectral content**

Now the effect of the pulse width, τ, on the high frequency components of the magnitude spectra of a trapezoidal pulse will be examined. Figure 17 shows the magnitude spectrum of a trapezoidal pulse with a rise time of .1 ns and a pulse width of 10 ns. Figure 18 displays the spectrum of another trapezoidal pulse with the same rise time (.1 ns) but a shorter pulse width (1 ns). At first glance, it appears that the spectral envelope of the shorter pulse would be much higher than that of the wider pulse at high frequencies, because its first corner frequency occurs at a higher frequency (318.3 MHz instead of 31.83 MHz). However, this

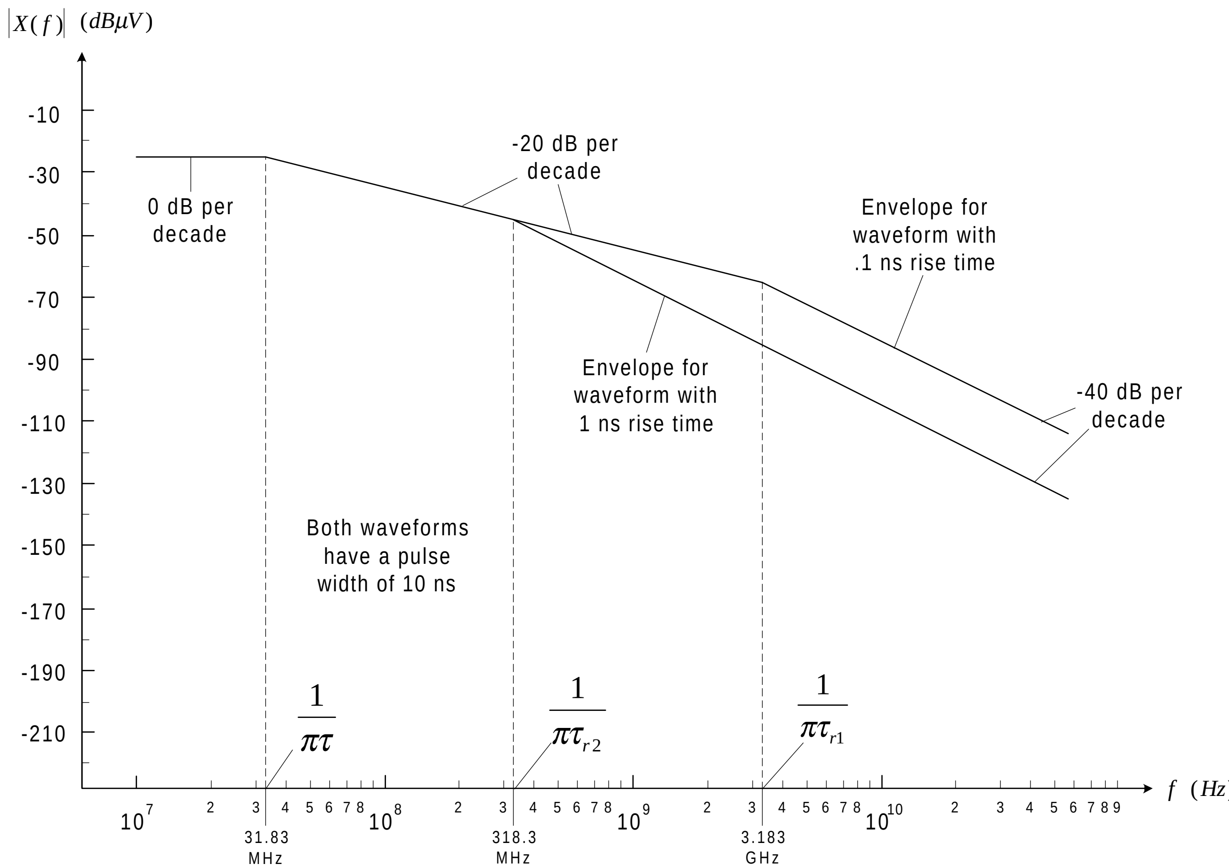

Figure 16: Envelopes of magnitude spectra of pulses with different rise times

the spectral envelope of the short pulse starts at about 20 dB below that of the 10 ns pulse. The envelopes of the magnitude spectra of both pulses meet at 318.3 MHz, as shown in Figure 19. Above 318.3 MHz, the spectral envelopes of both signals are very similar. Therefore, the high frequency content of a trapezoidal pulse is determined more by its rise and fall times than by its pulse width.

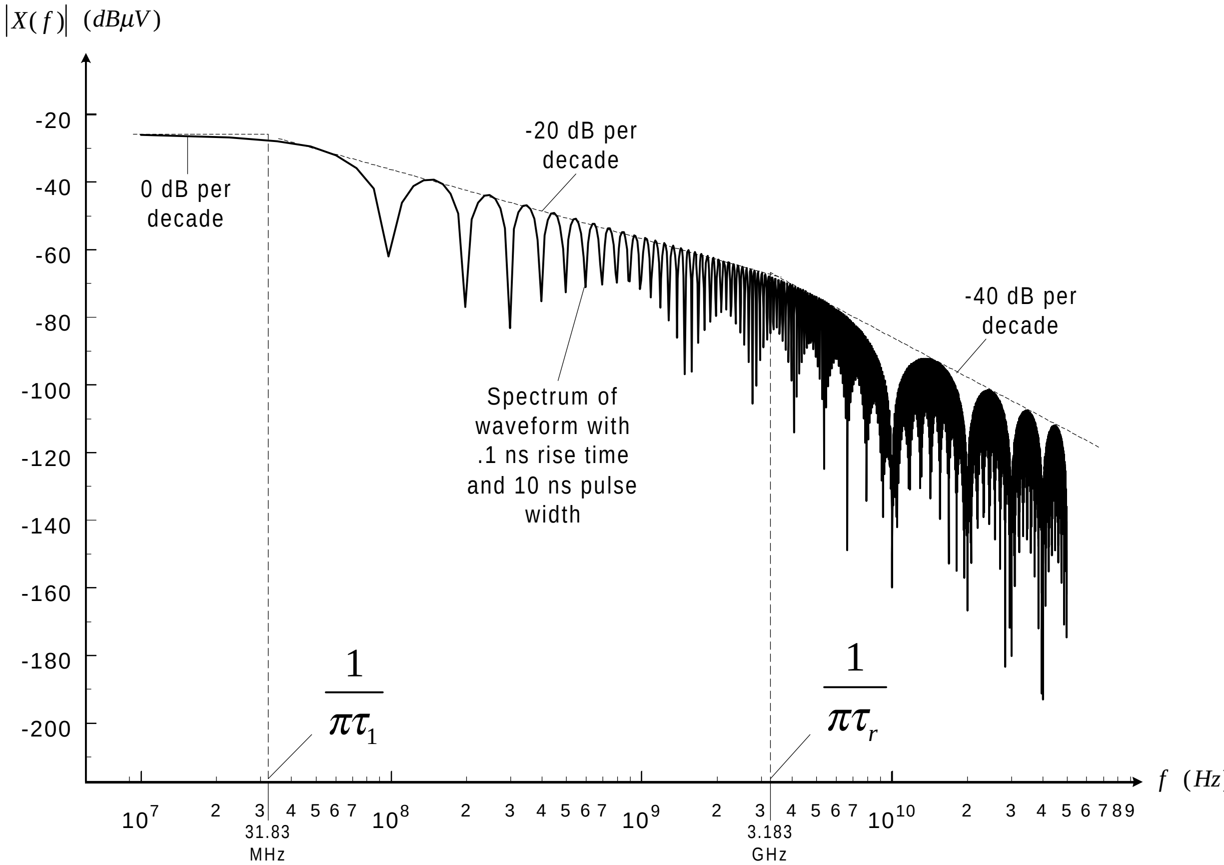

Figure 17: Magnitude spectrum of pulse with a .1 ns rise time and 10 ns pulse width

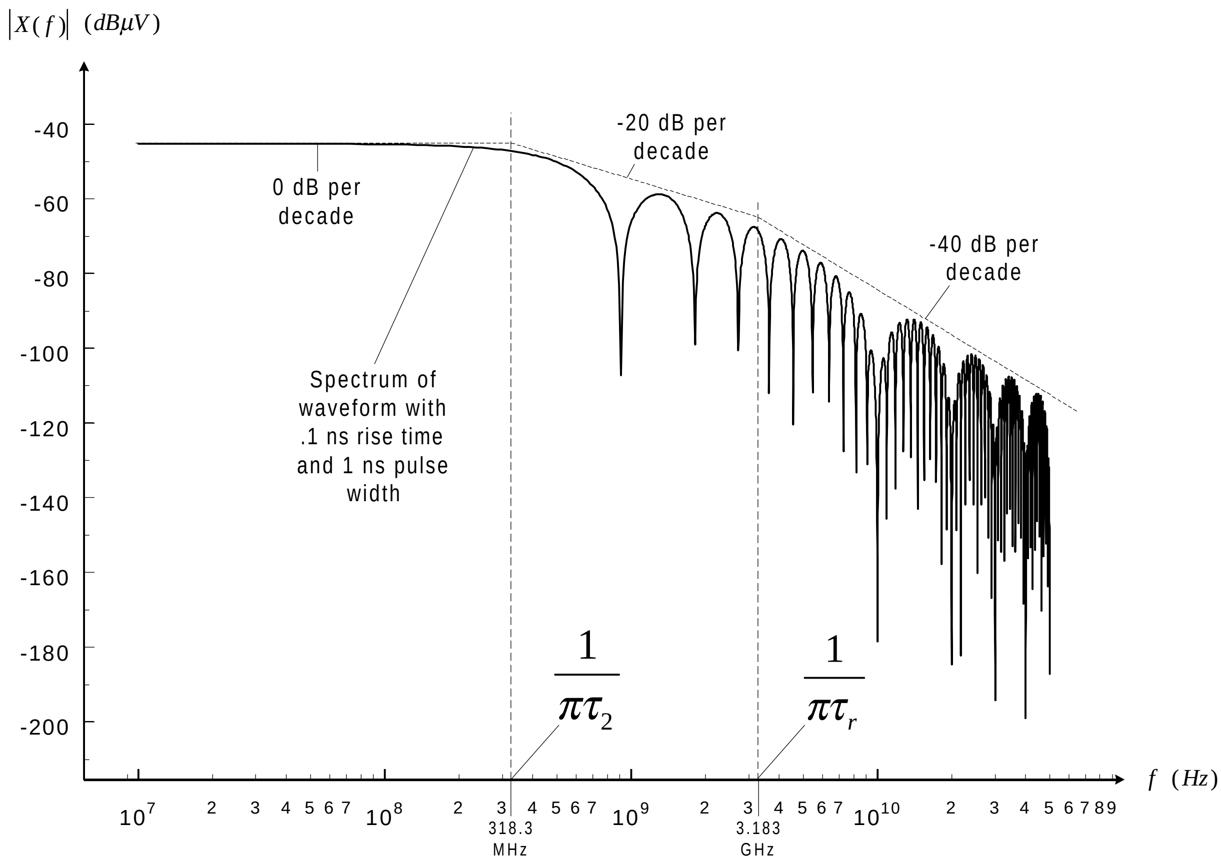

Figure 18: Magnitude spectrum of pulse with a .1 ns rise time and 1 ns pulse width

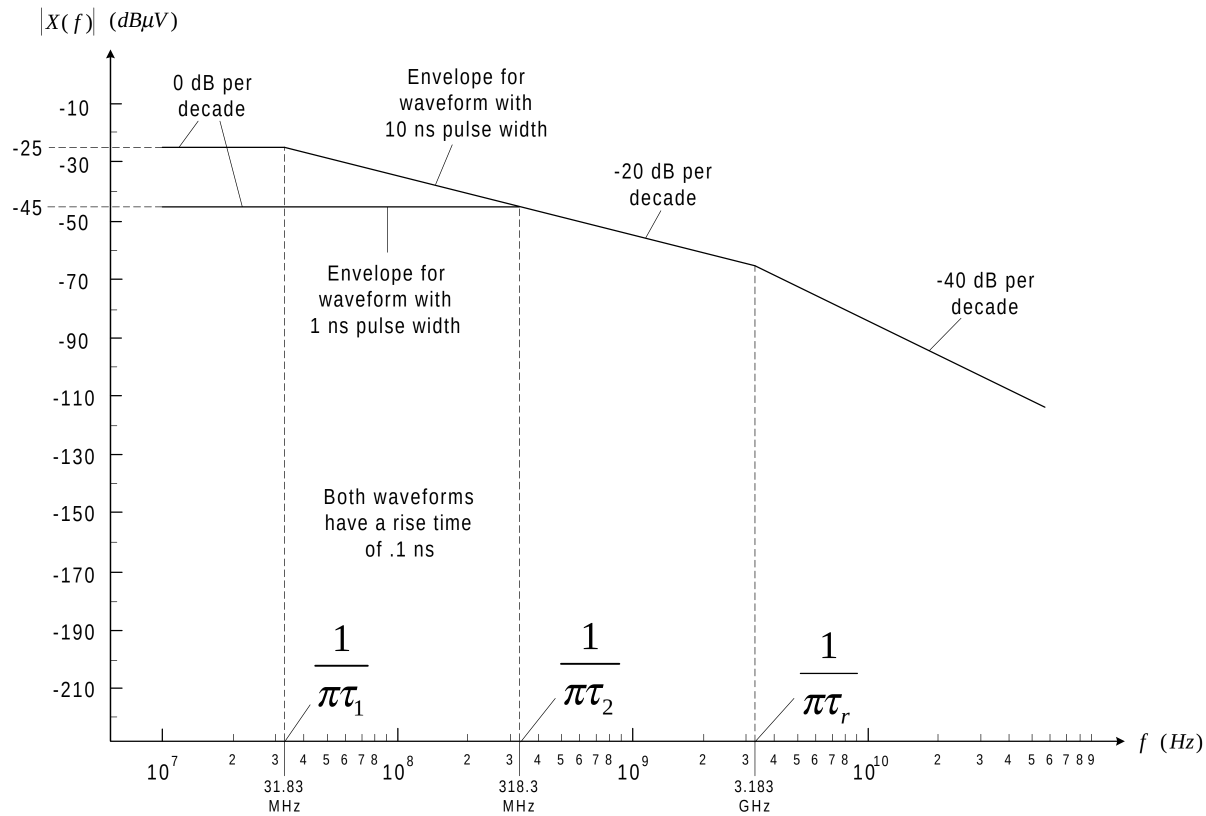

Figure 19: Envelopes of magnitude spectra of pulses with different pulse widths